

**Composition and activity of antifungal lipopeptides produced by *Bacillus* spp. in *daqu* fermentation**

Zhen Li<sup>a</sup>, Kleinberg X. Fernandez<sup>b</sup>, John C. Vederas<sup>b</sup>, Michael G. Gänzle<sup>a#</sup>

<sup>a</sup> *University of Alberta, Department of Agricultural, Food and Nutritional Science, T6G 2P5  
Edmonton, Alberta, Canada*

<sup>b</sup> *University of Alberta, Department of Chemistry, Edmonton, Alberta, T6G 2G2 Canada*

Declarations of interest: none

# corresponding author,

Michael G. Gänzle,

University of Alberta,

Dept. of Agricultural, Food and Nutritional Science,

4-10 Ag/For Centre,

Edmonton, AB,

Canada, T6G 2P5

Tel: + 1 780 492 0774

Email: [mgaenzle@ualberta.ca](mailto:mgaenzle@ualberta.ca)

1 **Abstract**

2 *Daqu* is a solid-state fermentation and saccharification starter for the Chinese liquor *baijouw*. During  
3 the *daqu* stage, amylolytic and proteolytic enzymes are produced by *Bacillus* and fungi. *Bacillus*  
4 spp. also produce lipopeptides with a broad spectrum of antimicrobial activities but direct evidence  
5 for their impact on community assembly in *daqu* is lacking. This study aimed to study the  
6 interaction between *Bacillus* spp. and fungi in *daqu* models. The antifungal activity of surfactin,  
7 fengycin, and iturin A was initially assessed *in vitro*. Iturin A displayed the strongest antifungal  
8 activity (MIC=10-50 mg/L). *In situ* antifungal activity of *B. amyloliquefaciens* and *B. velezensis*  
9 against molds was observed in a simple *daqu* model inoculated with single strains of *Bacillus*  
10 species. Formation of lipopeptides *in situ* was supported by quantification of mRNA encoding for  
11 enzymes for surfactin, fengycin, and iturin A biosynthesis. *In situ* antifungal activity of *Bacillus*  
12 species was also observed in a complex *daqu* model that was inoculated with 8 bacterial or fungal  
13 strains plus one of the three strains of *Bacillus*. A relationship of lipopeptides to *in situ* antifungal  
14 activity was supported by detection of the lipopeptides by liquid chromatography coupled to mass  
15 spectrometry. Both results indicated that *B. velezensis* FUA2155 had higher antifungal activity in  
16 the *daqu* model, and was the only strain that produced multiple iturin A congeners *in situ*. Taken  
17 together, this study provides evidence that production of lipopeptides by *Bacillus* species in *daqu*  
18 may impact community assembly and hence product quality.

19 **Keywords:** *Bacillus*; *daqu* fermentation; antifungal lipopeptides; mass spectrometry.

20

## 21 **1 Introduction**

22 Chinese liquor (*baijiu*) is a distilled liquor and one of the most popular alcoholic beverages in  
23 China (Zheng and Han, 2016). Chinese liquor is made with sorghum, wheat, rice, barley, or corn  
24 (Zheng et al., 2011; Zheng and Han, 2016). Differing from alcoholic cereal fermentations in Africa  
25 and Europe, where malt is used as a source of enzymes, hydrolytic enzymes are provided by  
26 microbial saccharification cultures including *daqu*, which is produced by spontaneous  
27 fermentation of cereals (Gänzle, 2022; Jin et al., 2017; Marco et al., 2021). *Baijiu* also differs from  
28 Japanese sake, which uses back-slopped *koji* with domesticated strains of *Aspergillus oryzae* as  
29 main or sole fermentation organism (Gibbons et al., 2012). The fermentation process of Chinese  
30 liquor consists of two stages: production of the saccharification starter *daqu* and the mash  
31 fermentation for ethanol production (He et al., 2019; Huang et al., 2017). *Daqu* has been divided  
32 into three categories: low-, medium-, and high-temperature *daqu*, which are used to produce  
33 Chinese liquor with light flavor, soy sauce flavor and strong flavor, respectively (Sakandar et al.,  
34 2020). The medium-temperature *daqu* is the most widely used starter in the production of  
35 traditional Chinese *baijiu* (Xiao et al., 2017).

36 The composition of microorganisms in *daqu* consists of bacteria, mycelial fungi and yeasts (Chen  
37 et al., 2021). Bacterial species include *Bacillus* spp., *Enterobacteriaceae* and *Lactobacillaceae*.  
38 *Bacillus* species are endophytes of plants and thus invariably present in the raw materials of *daqu*  
39 preparation (Ferreira et al., 2021; Leite et al., 2013), and are consistently found to be the dominant  
40 species throughout the fermentation (Chen et al., 2021; Wang et al., 2008; Zheng et al., 2013).  
41 Fungal strains consist of *Aspergillus* spp., *Mucor* spp., *Penicillium* spp., with *Aspergillus* spp.  
42 being dominant (Deng et al., 2021; Wang et al., 2008). *Saccharomyces* spp. are most frequently  
43 isolated yeasts (Wang et al., 2008).

44 *Daqu* is produced using unsterilized raw materials in an open environment without starter culture  
45 or inoculum and fermentation organisms are derived from the raw material or the environment.  
46 *Bacillus* spp. form stable associations with plants in the rhizosphere or as endophytes (Robinson  
47 et al., 2016; Shahzad et al., 2016), and thus are invariably present in cereal grains (Li et al., 2020).  
48 The shape of the *daqu* blocks provides a large surface area to support the growth of the aerobic  
49 bacilli, and the low moisture content slows the growth of *Enterobacteriaceae* and lactic acid  
50 bacteria (Zheng and Han, 2016). These ecological parameters thus allow *Bacillus* spp. to dominate  
51 throughout the production process (Zheng et al., 2013). Endospores formed by *Bacillus* remain  
52 active at low moisture content and high-temperature conditions (Setlow, 2006), supporting their  
53 presence as the most frequently isolated bacteria from *daqu*.

54 During the *daqu* production, hydrolytic enzymes including amylolytic enzymes are produced by  
55 bacteria and fungi (Li et al., 2014; Liu et al., 2018). Of the bacterial fermentation organisms,  
56 *Bacillus* spp. are the major group producing extracellular amylolytic enzymes (Li et al., 2014; Liu  
57 et al., 2018). The amylolytic system have been identified in genomes of *Bacillus* spp. (Li et al.,  
58 2020). Amylases produced in *daqu* are the major contributors to starch liquefaction and  
59 saccharification in the subsequent mash fermentation (Li et al., 2015). In addition, proteolytic  
60 enzymes produced by fungi and bacilli generate amino acids as precursors for synthesis of volatile  
61 flavor compounds in the mash stage (Liu et al., 2018).

62 *Bacillus* spp. also produce a wide range of lipopeptides with antimicrobial activity (Cochrane and  
63 Vederas, 2016; Zhang et al., 2022). These lipopeptides are produced by polyketide synthases  
64 (PKSs) and nonribosomal peptide-synthetases (NRPS) (Roongsawang et al., 2010). Lipopeptides  
65 produced by *Bacillus* spp. can be broadly grouped into three families: surfactins, fengycins and  
66 iturins (Cochrane and Vederas, 2016). These antifungal lipopeptides inhibit or kill fungi either by

67 inhibiting mycelial growth, affecting spore germination, or causing the hyphae or spores to swell  
68 or to lyse (Li et al., 2021). Genes coding for synthesis of antimicrobial lipopeptides including *bioA*,  
69 *bmyB*, *ituC*, *fenD*, *srfAA*, *srfAB*,  *yngG*, and *yndJ*, were identified in the genomes of bacilli isolated  
70 from *daqu* (Wu et al., 2021). In addition, *Bacillus* lipopeptides were identified in both *daqu* and  
71 *baijiu* (Chen et al., 2020; Zhang et al., 2014). For example, surfactin accumulated to a  
72 concentration of more than 7 mg/kg in the *daqu* stage of *baijiu* fermentation and was diluted to  
73 1.5 mg/kg by the addition of cooked cereals at the mash stage. The concentration of the non-  
74 volatile peptide in the distilled end product was less than 1 µg/L (Chen et al., 2020). It remains  
75 unknown, however, whether the production of antifungal lipopeptides in *daqu* impact community  
76 assembly in *daqu* and mash fermentations. It was therefore the aim of this study to investigate the  
77 role of antifungal lipopeptides produced by *Bacillus* species on community assembly in *daqu*.

## 78 **2 Materials and methods**

### 79 **2.1 Strains used in this study and preparation of the inocula**

80 The origin and growth conditions of strains used in this study are listed in Table 1. LB broth  
81 (SigmaAldrich, ON, Canada) was inoculated with a single colony of *Bacillus amyloliquefaciens*  
82 Fad We, *B. amyloliquefaciens* Fad 82, *Bacillus velezensis* FUA2155, or *Kosakonia cowanii*  
83 FUA10121 and incubated overnight at 37 °C at 200 rpm agitation. *Weissella cibaria* FUA3456  
84 cultures was prepared in a similar manner but the strain was grown in modified MRS (mMRS)  
85 broth (Gänzle et al., 1998) at 30 °C for 2 d without agitation.

86 Spore suspensions of the following fungal strains, *Aspergillus niger* FUA5001,  
87 *Aspergillus clavatus* FUA5004, *A. clavatus* FUA5005, *Mucor racemosus* FUA5009, and  
88 *Penicillium roqueforti* FUA5012 were prepared as described (Zhang et al., 2010). In brief, the  
89 strains were cultivated on malt extract agar (MEA, SigmaAldrich, ON, Canada) plates at 25 °C for

90 7 d. Conidia were collected from agar plates by adding 10 mL of sterile distilled water and  
91 harvesting of fungal biomass with an L-shaped cell spreader (Fisher Scientific, Ottawa, Canada).  
92 The spore suspensions were filtered to eliminate mycelial cells and spores were harvested by  
93 centrifugation. Spores were quantified with a haemocytometer (Fein-Optik, Jena, Germany).  
94 Inocula of *Saccharomyces cerevisiae* FUA4002, *Saccharomycopsis fibuligera* FUA4036, and  
95 *Pichia kudriavzevii* FUA4039 were prepared by inoculating malt extract broth (MEB,  
96 SigmaAldrich, ON, Canada) with single colonies, followed by incubation for 2 d at 30 °C. The  
97 cell counts were confirmed with a hemocytometer.

## 98 **2.2 *In silico* prediction of lipopeptides produced by *Bacillus* spp.**

99 The genome sequences of *Bacillus* strains (Li et al., 2019) were used to identify biosynthetic gene  
100 clusters for antimicrobial secondary metabolites using the bacterial version of the antiSMASH  
101 (Blin et al., 2021). Identification of gene clusters encoding different lipopeptides in the genomes  
102 of *B. amyloliquefaciens* Fad We, *B. amyloliquefaciens* Fad 82 and *B. velezensis* FUA2155 were  
103 verified by BLAST on NCBI. All gene clusters identified by antiSMASH were used as query  
104 sequences for BLASTn against the NCBI nucleotide database.

## 105 **2.3 Extraction and purification of the antifungal peptides from LB cultures**

106 To study the antifungal peptides produced by *B. amyloliquefaciens* Fad We, *B. amyloliquefaciens*  
107 Fad 82 and *B. velezensis* FUA2155, the peptides were extracted from 150 mL of the stationary  
108 phase cultures in LB broth. The cultures were incubated at 37 °C, 200 rpm for 3 d and cells were  
109 removed by centrifugation at 12,000 × *g* for 20 min. The pH of the supernatants was adjusted to 2  
110 with 6M HCl, followed by incubation at 4 °C overnight. Solid crude lipopeptides were collected  
111 by centrifugation at 12,000 × *g* for 20 min, and the precipitate was extracted with methanol. The

112 organic solvent was evaporated *in vacuo* at 50 °C (Yang et al., 2015). The extracted peptides were  
113 dissolved in 1 mL methanol and filtered through 0.45 µm filters to remove solids.

#### 114 **2.4 Minimum inhibitory concentration assay**

115 The minimum inhibitory concentration (MIC) of surfactin, fengycin and iturin A was determined  
116 in a critical dilution assay. Iturin A and fengycin (Sigma-Aldrich, Oakville, Canada) and surfactin  
117 (MedChemExpress, Monmouth Junction, USA) were dissolved in DMSO to a concentration of  
118 5 g/L as stock solutions and stored at –80 °C until further use. The mycelial fungi *A. niger*  
119 FUA5001, *A. clavatus* FUA5004, *A. clavatus* FUA5005, *M. racemosus* FUA5009 and  
120 *P. roqueforti* FUA5012, as well as the yeasts, *S. cerevisiae* FUA4002, *S. fibuligera* FUA4036 and  
121 *P. kudriavzevii* FUA4039 were used as indicator strains. Inocula were prepared as described  
122 above. The growth was observed visually, and the MIC was recorded one day after visible growth.  
123 The MIC values were determined in three independent experiments using replicate preparations of  
124 the conidiospores. For each experiment, 90 µL of the lipopeptides iturin, surfactin, fengycin were  
125 mixed with MEB (for fungi) or mMRS broth (for yeasts) in a 96-well microtiter plate, followed  
126 by 2-fold serial dilutions with the respective growth medium to cover the concentration range of  
127 2.5 g / L to 2.5 mg / L. Each well was inoculated with 10 µL of spores or vegetative cells with a  
128 cell count of 10<sup>6</sup> CFU/mL. The controls contained the inocula but distilled water was used instead  
129 of the lipopeptide solutions.

#### 130 **2.5 Preparation of simplified *daqu* model**

131 The production of antifungal peptides by the three strains of *Bacillus* (*B. amyloliquefaciens*  
132 Fad We, *B. amyloliquefaciens* Fad 82 and *B. velezensis* FUA2155) was initially assessed in a  
133 simplified *daqu* model that were inoculated with only one *Bacillus* strain. Overnight cultures of  
134 the three *Bacillus* strains were prepared by inoculating single colonies in 100 mL LB broth that

135 was incubated at 37 °C and 200 rpm for 24 h. Cells were harvested by centrifugation and  
136 resuspended in sterile water to obtain a cell count of  $10^9$ - $10^{10}$  CFU/mL. One mL of this inoculum,  
137 60 g wheat flour and 30 mL sterile tap water were mixed in a sterile plastic bag, resulting in a  
138 water content of around 35 % and a final cell count of approximately  $10^7$ - $10^8$  CFU/g. Wheat flour  
139 mixed with sterile water without inoculation of strain of *Bacillus* served as the control. The *daqu*  
140 samples were manually pressed and shaped in Petri-dishes and incubated at controlled  
141 temperatures and relative humidity (rH) as follows: shaping stage, 30 °C, rH 95 % for 1 d; ripening  
142 stage, 37 °C, rH 95 % for 2 d; high-temperature stage, 55 °C, rH 90 % for 7 d; and maturation  
143 stage, 37 °C, rH 75 % for 6 d. This temperature and relative humidity profile matches conditions  
144 of medium-temperature *daqu* conditions (Zheng and Han, 2016). Samples were incubated in  
145 hermetically sealed containers and the relative humidity in these containers was controlled with  
146 the following saturated salt solutions: K<sub>2</sub>SO<sub>4</sub>, rH 95 %; KNO<sub>3</sub>, rH 90 %; NaCl, rH 75 %. After the  
147 high-temperature stage, the *daqu* samples were dry and microbial population remained stable, the  
148 incubation was therefore not extended for more than a total of 16 d.

## 149 **2.6 Determination of pH and total bacterial cell counts of the simplified *daqu* model, and** 150 **observation of mold growth**

151 To measure the pH and viable cell counts, 0.5 g samples were collected and diluted 10-fold with  
152 sterile 18 MΩ water. Samples were further diluted in peptone water and plated on LB agar. The  
153 pH of the first dilution was then measured with a glass electrode. The LB agar plates were  
154 incubated at 37 °C for 24 h prior to counting the total number of colonies per plate; differential  
155 cell counts of *Bacillus* species were also recorded based on the colony morphology.

156 Fungal growth during the simplified *daqu* model was observed daily and recorded as follows: –,  
157 no mycelial growth visible; +, small spots of mycelial growth; ++, spots of mycelial growth and



158 conidia; +++, 25-50 % of the surface covered by mycelium; and +++, more than 50 % of the  
159 surface covered by mycelium. Representative pictures defining the fungal growth are shown in the  
160 Supplementary Figure S1.

## 161 **2.7 Quantification of expression of genes encoding for synthesis of three antifungal** 162 **lipopeptides in the simplified *daqu* model by reverse transcription quantitative PCR** 163 **(RT-qPCR)**

164 To extract mRNA and prepare cDNA of the 1<sup>st</sup>, 2<sup>nd</sup>, and 3<sup>rd</sup> day of samples from the the simplified  
165 *daqu* model, aliquots of 0.5 g *daqu* were mixed with 3 mL RNAProtect Bacteria Reagent (Qiagen,  
166 Germantown, USA) and incubated for 10 min. The solids were then removed by centrifugation at  
167 500 × g for 10 min. The cells in the supernatant were harvested by centrifugation. The RNA was  
168 isolated from cell pellets using TRIzol LS reagent based on the manufacturer's instructions  
169 (ThermoFisher Scientific, Waltham, USA). Contaminant genomic DNA was digested by DNase  
170 treatment using the RQ1 RNase-Free DNase (Fisher Scientific), and cDNA libraries were  
171 generated by reverse transcription using the QuantiTect Reverse Transcription Kit (Qiagen).

172 To quantify the expression of genes encoding surfactin, fengycin and iturin A production in the  
173 *daqu* model, the genes *srfAA*, *fenA* and *ituA* encoding part of the nonribosomal peptide synthetase  
174 subunits of surfactin, fengycin and iturin A, respectively, were chosen. Primers used in qPCR are  
175 shown in Table 2 and the specificity of the primers was verified by PCR using chromosomal DNA  
176 of the three strains as a template. The single-copy gene *gyrB* which encodes for the DNA gyrase  
177 subunit B was used as the housekeeping gene for relative quantification of gene expression.

178 Gene expression was detected by QuantiFast SYBR Green PCR Kit (Qiagen) and reverse-  
179 transcriptase qPCR (7500 Fast, Applied Biosystems, Foster City, CA). Cells growing  
180 exponentially in LB broth (OD<sub>600nm</sub> 0.8) were used as reference conditions. Negative controls

181 included DNase-treated RNA and a no-template control. Gene expression relative to cultures in  
182 LB was calculated with the  $\Delta\Delta C_T$  method and  $\log_2$  transformed. Significant differences in the  
183 relative gene expression were assessed with a t-test and an error probability of 5 % ( $P < 0.05$ ).  
184 Data are presented as mean  $\pm$  standard deviation of three independent fermentations.

## 185 **2.8 Preparation of complex model of *daqu* fermentation**

186 To further study the role of antifungal peptides produced by *Bacillus* spp. in *daqu*, a complex *daqu*  
187 model was prepared by including one representative of major groups of fermentation organisms.  
188 In addition to inoculation with strains of *Bacillus*, cell or spore suspensions of *A. niger* FUA5001,  
189 *M. racemosus* FUA5009, and *P. roqueforti* FUA5012, *S. cerevisiae* FUA4002, *S. fibuligera*  
190 FUA4036, and *P. kudriavzevii* FUA4039 were added to a final cell count of  $10^5$  CFU/g each. Cell  
191 suspensions of *K. cowanii* FUA10121 and *W. cibaria* FUA3456 were added to a final cell count  
192 of  $10^6$  CFU/g each. The samples from the complex *daqu* model were prepared and incubated at the  
193 same conditions with the simplified *daqu* model as described above.

## 194 **2.9 Determination of microbial population in the complex model of *daqu* by qPCR**

195 Samples from the complex *daqu* model were collected after 1, 3, 6, 10, 13 or 16 days of  
196 fermentation were collected. Community DNA was extracted by E.Z.N.A. Soil DNA Kit (Omega  
197 Bio-tek, Inc. Norcross, USA) according to the manufacturer's instructions. The absolute quantities  
198 of microbial populations were determined with qPCR using primers targeting *Bacillus* species, all  
199 bacteria, and fungi with the primer pairs *srfAAF* and *srfAAR*, 340F and 758R (Juck et al., 2000),  
200 and *Fnpstr* and *Rnpstr*, respectively (Rodríguez et al., 2012). The assays were carried out on a 7500  
201 Fast instrument (Applied Biosystems) with a commercial QuantiFast SYBR Green PCR kit  
202 (Qiagen) according to the manufacturer's instructions. The calibration curves and amplification  
203 conditions were constructed as described elsewhere (Metzler-Zebeli et al., 2010). In short, the PCR

204 amplicons was amplified with chromosomal DNA from *B. velezensis* or *A. niger* FUA5001, and  
205 purified. The DNA concentration of the amplicons was measured with a Nanodrop UV/Vis  
206 spectrophotometer (Thermofisher) to calculate the copy number, and the DNA solutions were  
207 diluted in serial tenfold dilutions to exhaustion. The diluted DNA solutions were used as template  
208 for qPCR to establish the calibration curves.

## 209 **2.10 Extraction and purification of lipopeptides from the complex *daqu* model**

210 To monitor the production of antifungal lipopeptides in the complex *daqu* model, samples were  
211 obtained on the 1<sup>st</sup>, 3<sup>rd</sup>, 6<sup>th</sup>, 10<sup>th</sup>, 13<sup>th</sup>, and 16<sup>th</sup> day of incubation. The extraction procedure for  
212 lipopeptides was similar to that described above for extraction from LB cultures but with an  
213 additional homogenization step. Approximately 8.5 g of the *daqu* samples were homogenized in  
214 50 mL distilled water by stomaching for 5 minutes. The samples were then centrifuged at  
215 12,000 × *g* for 20 min to remove solids. Samples were further processed with same procedure as  
216 described above for cultures in LB.

## 217 **2.11 Antifungal activity test of peptides produced by *Bacillus* in the complex *daqu* model**

218 To determine the production of antifungal peptides in the complex *daqu* model, the antifungal  
219 activity of methanolic *daqu* extracts was determined with *A. niger* FUA5001 as the indicator strain.  
220 Serial 2-fold dilutions of the peptide extracts and MEB were prepared in 96-well microtiter plates  
221 and inoculated with 10 μL of a suspension of conidia *A. niger* FUA5001 to a cell count of  
222 10<sup>6</sup> CFU/mL. The plates were then incubated at 25 °C for 5 d. After incubation, fungal growth was  
223 observed visually.

## 224 **2.12 Procedure for LCMS analysis of LB culture and complex model of *daqu* extracts**

225 To qualitatively identify the antifungal lipopeptides produced by *B. amyloliquifaciens* Fad We,  
226 *B. amyloliquifaciens* Fad 82, and *B. velezensis* FUA2155, each sample was detected first by  
227 reverse phase-high performance liquid chromatography followed by coupled to using mass  
228 spectrometry (RP-HPLC-MS). Analysis was performed using an Agilent 1200 SL HPLC System  
229 with a Phenomenex Aeris XB-C8 column, 3.6  $\mu\text{m}$ , 100  $\text{\AA}$ , 50 x 2.1 mm with a trap cartridge  
230 (Phenomenex, Torrance, USA) with a guard thermostated at 35  $^{\circ}\text{C}$ . A buffer gradient composed  
231 of 0.1 % formic acid in water (mobile phase A) and 0.1 % formic acid in acetonitrile (mobile phase  
232 B) was used. A 2  $\mu\text{L}$  aliquot of the sample was loaded onto the column at a flow rate of  
233 0.45 mL/min and an initial buffer composition of 95 % mobile phase A and 5 % mobile phase B  
234 for 0.5 min was performed to effectively remove the salts. The elution of the lipopeptides was  
235 performed using a linear gradient from 5 % to 65 % mobile phase B for 4.8 min, 65 % to 95 %  
236 mobile phase B for 1.0 min, 95 % mobile phase B for 0.8 min, then back to the initial buffer  
237 conditions in 0.5 min. Mass spectra were acquired in a positive mode of ionization using an Agilent  
238 6220 Accurate-Mass TOF HPLC/MS system (Santa Clara, CA, USA), equipped with a dual  
239 sprayer electrospray ionization source; the second sprayer providing a reference mass solution.  
240 Mass correction was performed for each individual spectrum using peaks at  $m/z$  121.0509 and  
241 922.0098 from the reference solution. The conditions for mass spectrometry are as stated: drying  
242 gas 10 L/min at 350  $^{\circ}\text{C}$ , nebulizer at 30 psi, mass range of 100-3200 Da, acquisition rate of  $\sim 1.03$   
243 spectra/sec, fragmentor voltage at 175 V, skimmer voltage at 65 V, capillary voltage at 4000 V,  
244 and instrument state 2 GHz High Dynamic Range. Data analysis was performed using the Agilent  
245 MassHunter Qualitative Analysis software package version B.07.00 SP2.

## 246 3 Results

### 247 3.1 Prediction of antimicrobial lipopeptides produced by *B. amyloliquefaciens* and 248 *B. velezensis*

249 The production of antimicrobial peptides in the genomes of *B. amyloliquefaciens* Fad We,  
250 *B. amyloliquefaciens* Fad 82 and *B. velezensis* FUA2155 was initially predicted by antiSMASH  
251 (Supplementary Table S1). All three strains were predicted to produce several antimicrobial  
252 lipopeptides. The predicted number and percent sequence identity of peptides in the two strains of  
253 *B. amyloliquefaciens* were identical. *B. velezensis* FUA2155 was predicted to additionally produce  
254 three antimicrobial peptides including a second surfactin gene cluster. The genome of *B. velezensis*  
255 FUA2155 also included gene clusters encoding for the synthesis of the antibacterial peptides  
256 difficidin and macrolactin H with high identity. Difficidin has both antifungal and antibacterial  
257 activities (Im et al., 2020), while macrolactins have broad-spectrum antimicrobial activity (Yuan  
258 et al., 2016). Macrolactin H exhibited antibacterial activity (MIC = 10 mg/L) against  
259 *Staphylococcus aureus* (Nagao et al., 2001) but antifungal activity has not been described.

260 Predictions of the antifungal peptides by antiSMASH were verified by BLASTn (Supplementary  
261 Table S2). No significant similarity was found for butirosin A/B and the query coverage for  
262 bacillibactin, bacilysin and fengycin biosynthetic genes in the genomes of the three *Bacillus* strains  
263 were below 60 %. The query coverage and identity of bacillaene, surfactin and iturin in the three  
264 strains were above 60 % (Supplementary Table S2). Based on the presence of gene clusters for  
265 antimicrobial lipopeptides, and literature data on their antifungal activity, the peptides surfactin,  
266 iturin and fengycin were selected for subsequent experiments.

### 267 **3.2 Analysis of antifungal lipopeptides in the LB cultures of *Bacillus***

268 To determine whether the presence of gene clusters coding for production of three families of  
269 antifungal lipopeptides surfactin, fengycin and iturins lipopeptides result in production of these  
270 lipopeptides during growth in LB broth, total lipopeptides were extracted from LB culture  
271 supernatants of *B. amyloliquefaciens* Fad We, *B. amyloliquefaciens* Fad 82 and *B. velezensis*  
272 FUA2155. Signal intensities of surfactin, iturin A, and fengycin were qualitatively analyzed by  
273 HPLC-MS, and the log[signal intensities] are shown in a gradient (Figure 1). Of the three families  
274 of lipopeptide tested, surfactins were detected in all three strains of *Bacillus* with a high signal  
275 intensity. In LB cultures of *B. amyloliquefaciens* Fad 82, the signal intensity of most surfactin  
276 congeners were several orders of magnitude lower than that of the other two strains. Iturins were  
277 also produced by all three strains but the log[signal intensities] in extracts from cultures of  
278 *B. amyloliquefaciens* Fad We, and Fad 82 was about 100 times lower than that in the *B. velezensis*  
279 FUA2155 extracts. Fengycins were not detected in any of the cultures.

### 280 **3.3 Antifungal activity of surfactin, fengycin, and iturin A**

281 The minimum inhibitory concentration of commercial surfactin, fengycin and iturin A was  
282 determined with a critical dilution assay with five mycelial fungi and three yeasts as indicator  
283 strains. Iturin A inhibited 7 of the 8 indicator strains with an MIC ranging from 10 to 50 mg/L;  
284 only *S. fibuligera* was relatively resistant (Figure 2). The MIC of surfactin and fengycin against  
285 most indicator strains ranged from 300 to 500 mg/L, the highest concentration that was tested.  
286 Fengycin inhibited *M. racemosus* FUA5009 and *S. cerevisiae* FUA4002 at a concentration of  
287 about 200 mg/L.

### 288 3.4 Performance of *Bacillus* as starter cultures in simplified *daqu* model

289 Of the three strains of *Bacillus* applied in this study, *B. velezensis* FUA2155 was isolated from  
290 *daqu* (Wang et al., 2018), while the two strains of *B. amyloliquefaciens* were isolated from ropy  
291 bread (Röcken and Spicher, 1993). All three encode for multiple amylases, which were shown to  
292 hydrolyse starch during storage of bread (Li et al., 2020), but are beneficial technological traits in  
293 *daqu*. To determine their suitability as cultures for *daqu*, the performance of the three strains was  
294 evaluated in a simplified *daqu* model using un-inoculated wheat flour as a control. The change of  
295 the pH and the viable cell counts during the fermentation are shown in Figure 3 and Figure 4,  
296 respectively. A decrease of pH from 6.5 to lower than 5.5 was observed in the four *daqu* models,  
297 including the control. The pH increased in samples inoculated with *B. velezensis* FUA2155 during  
298 the ripening stage.

299 The total cell counts during the simplified *daqu* model are illustrated in Figure 4. *B. velezensis*  
300 FUA2155 and *B. amyloliquefaciens* Fad We showed high cell counts of approximately 8  
301 log(CFU/mL) after the shaping stage and remained consistent until the end of the fermentation.  
302 Cell counts of samples inoculated with *B. amyloliquefaciens* Fad 82 dropped sharply after the  
303 ripening stage, and a similar trend was observed in the control.

304 An initial assessment of whether the inocula persisted relative to flour-derived microorganisms,  
305 was based on the observation of colony morphology on LB agar plates. In uninoculated control  
306 samples, colonies with a morphology that matched the strains of *Bacillus* that were used as  
307 inoculum accounted for less than 10 % of the total colonies throughout incubation. In samples  
308 inoculated with *B. amyloliquefaciens* Fad 82, about 70 % of colonies had the same morphology as  
309 the inoculum. In samples inoculated with *B. amyloliquefaciens* Fad We or *B. velezensis* FUA2155,  
310 more than 90 % of the colonies had the same morphology as the inoculum. Taken together, cell

311 counts in combination with observation of the colony morphologies and the quantification of gene  
312 expression (see below) suggest that *B. amyloliquefaciens* Fad We and *B. velezensis* FUA2155 were  
313 the dominant fermentation microbiota in the simplified *daqu* models.

314 In addition to bacterial growth, the growth of mycelial fungi was observed on the surface of *daqu*  
315 samples (Table 3). Substantial mold growth was observed in the uninoculated control samples at  
316 day 2 and mycelia covered most of the surface by day 3. Mold growth on samples inoculated with  
317 *B. amyloliquefaciens* Fad 82 was comparable to the control. Mold growth and formation of conidia  
318 was not detected on samples inoculated with *B. amyloliquefaciens* Fad We until day 4, while no  
319 visible mold growth was observed on samples inoculated with *B. velezensis* FUA2155. On day 4,  
320 samples were transferred to 55 °C which inhibited any further growth of molds irrespective of the  
321 inoculum (Table 3).

### 322 **3.5 Gene expression of *srfAA*, *fenA* and *ituA* on the first, second, and third day of the** 323 **simplified *daqu* model**

324 To determine whether antifungal lipopeptides are expressed during the growth of *Bacillus* in the  
325 simplified *daqu* model, mRNA encoding for *srfAA*, *fenA* and *ituA* was quantified in the samples  
326 of simplified *daqu* model by RT-qPCR (Figure 5). Relative gene expression was calculated with  
327 *gyrB* as the housekeeping gene and exponential cultures in LB broth as reference conditions. All  
328 three genes were expressed by all three strains during growth in the simplified *daqu* model. Over-  
329 expression of *srfAA* and *fenA* was observed at day 1 and/or day 2 of fermentation. On day 3 of  
330 fermentation, *srfAA* was down-regulated in all three strains. *B. amyloliquefaciens* FAD 82 also  
331 down-regulated *fenA* and *ituA* on day three of incubation (Figure 5). Taken together, the expression  
332 of *srfAA*, *fenA* and *ituA* indicates that the corresponding lipopeptides may be present in *daqu*.



### 333 **3.6 Antifungal activity of peptides produced by *Bacillus* in the complex *daqu* model**

334 To provide direct evidence for production of antifungal lipopeptides in the complex *daqu* model,  
335 extracts were analysed with respect to their antifungal activity and the presence of surfactin, iturin  
336 A, and fengycin. The results of antifungal activity test of antifungal lipopeptides extracted from  
337 the complex *daqu* model are illustrated in Table 4. *A. niger* FUA5001 was used as the indicator  
338 strain to assess the antifungal activity of extracts from the complex *daqu* model. Extracts from the  
339 control samples inoculated with all 8 fermentation organisms, but not with any *Bacillus* strains,  
340 did not inhibit mold growth, indicating that bacilli were the sole or main contributors to antifungal  
341 activity. The inhibitory activity of *daqu* extracts obtained after 1 d of incubation was highly  
342 variable. Extracts from *daqu* inoculated with *B. velezensis* FUA2155 showed strong and consistent  
343 antifungal activity from the 1<sup>st</sup> to the 6<sup>th</sup> day of incubation. During this period, consistent antifungal  
344 activity was also observed for extracts obtained from *daqu* samples that were inoculated with the  
345 two strains of *B. amyloliquefaciens*. However, the inhibitory activity was weaker when compared  
346 to samples with *B. velezensis* FUA2155.

347 To confirm the persistence and antifungal activity of the inoculated *Bacillus* strains, gene copies  
348 representing *Bacillus*, total bacteria, and fungi in the complex *daqu* model were quantified by  
349 qPCR (Supplementary Figure S2). An increase of *Bacillus*, bacteria and fungi was found in each  
350 sample in the ripening stage (1<sup>st</sup> to 3<sup>rd</sup> day). *B. velezensis* FUA2155 showed the highest  
351 log(copies/g) of *Bacillus* and total bacteria and the lowest log(copies/g) of fungi during the whole  
352 process. The log(copies/g) of total bacteria count for *B. amyloliquefaciens* Fad We and Fad 82  
353 from the 3<sup>rd</sup> to 10<sup>th</sup> day of fermentation ranged from 11-12 but decreased on the 13<sup>th</sup> day.  
354 Additionally, log(copies/g) of fungi remained stable after the 3<sup>rd</sup> day. Overall, the gene copies of  
355 *Bacillus*, total bacteria, and fungi were different among the complex *daqu* samples inoculated with

356 different *Bacillus* strains and *B. velezensis* FUA2155 showed competitive growth compared to the  
357 other two *Bacillus* strains.

### 358 **3.7 Analysis of antifungal lipopeptides in extracts from the complex *daqu* model by LC-** 359 **MS/MS**

360 To further compare the production of the lipopeptides from the three strains of *Bacillus* in *daqu*,  
361 the extracts of the complex *daqu* model were also analyzed for the presence of antifungal  
362 lipopeptides. The signal intensity of the lipopeptides extracted from different time points of  
363 incubation were qualitatively detected by LC-MS/MS, and the log[signal intensity] of surfactin,  
364 iturin A, and fengycin are shown in Figure 6.

365 The signal intensity of surfactin, iturin A, and fengycin in the different *daqu* samples were variable.  
366 Fengycin was not detected in any of the samples. Some surfactin congeners were detected among  
367 all the samples including the control group. Because the grains used as substrate contained *Bacillus*  
368 (Figure S2), low levels of the lipopeptides can be expected (Figure 6). The signal intensity of  
369 surfactins C52-C55 in *B. amyloliquefaciens* Fad We samples from day 1 to day 10 was relatively  
370 high. Surfactin C50-C55 had the highest intensity of surfactins in *B. velezensis* FUA2155 samples  
371 from day 3 to day 10. The log[signal intensity] of iturins, on the other hand, demonstrated a  
372 substantial difference. Iturin A C47-C51 was found in all *B. velezensis* FUA2155 samples. No  
373 iturin A C47 was found in any of the samples fermented with *B. amyloliquefaciens* Fad We. The  
374 signal strength of iturins was low or below detection limit in *B. amyloliquefaciens* Fad 82 and  
375 control samples.

## 376 4 Discussion

377 Experimentation described in this communication expands prior knowledge by providing a  
378 comprehensive qualitative analysis of congeners of surfactin, iturin A, and fengycin from *daqu*  
379 models, as well as by documenting *in situ* antifungal activity in simple and complex *daqu* models.  
380 Previous studies discovered only one or two peptides in *jiuqu/baijiu* samples and did not verify  
381 their biological activity (Chen et al., 2020; Zhang et al., 2014). Moreover, current information of  
382 the contribution of the diverse microbes in *daqu* to enzymatic and microbial conversions is largely  
383 based on correlation of sequence data to metabolome data in uncontrolled, spontaneous  
384 fermentations (Deng et al., 2021; Huang et al., 2017; Xiao et al., 2017). Our study complements  
385 these past studies by targeted analysis of *daqu* models that were inoculated with one or several  
386 strains for antifungal activity and the presence of lipopeptides. Results indicate that the production  
387 of different lipopeptides by bacilli *in situ* influences the community assembly and may hence  
388 impact the flavor of *baijiu*. The implications of the antifungal activity of bacilli on the quality of  
389 *baijiu*, however, remain to be demonstrated in future studies.

390 Numerous strains of *Bacillus* spp. have been developed as biological control agents of plant and  
391 pathogens (Schirawski and Perlin, 2018). Strains of *Bacillus* occur as endophytes which produce  
392 antimicrobial peptides to protect the plants against harmful microbes (Shahzad et al., 2016).  
393 Therefore, the presence of *Bacillus* endospores in *daqu* relates to the stable occurrence of these  
394 organisms as part of commensal microbiota of plants, including wheat (Fan et al., 2011), and to  
395 the formation of spores which remain viable throughout storage and processing of grains.  
396 Correspondingly, cereal grains, flours and cereal foods generally harbor spores of *Bacillus* species  
397 (Needham et al., 2005) which makes their presence in *daqu* as well as bread predictable. The *daqu*  
398 isolate *B. velezensis* FUA2155 and the bread isolate *B. amyloliquefaciens* Fad 82 performed

399 equally well in the simple and complex *daqu* models, further indicating that the establishment  
400 niche (wheat) and not the source of isolation – *daqu* versus bread – is relevant for strain selection  
401 and performance.

402 Lipopeptides synthesized by *Bacillus* strains possess broad-spectrum antimicrobial activity.  
403 Different lipopeptides have unique chemical structures and biological activities (Cochrane and  
404 Vederas, 2016). Surfactins are powerful biosurfactants with emulsifying properties. Because of  
405 the amphiphilic nature, surfactins are tightly anchored into lipid layers and can thus interfere with  
406 biological membrane integrity. Surfactins have antibacterial and antiviral abilities, but no  
407 apparent antifungal effects (Ongena and Jacques, 2008).

408 Iturins exhibit strong *in vitro* antifungal activity against yeast and fungi but only limited  
409 antibacterial and no antiviral activities (Aranda et al., 2005). For example, iturins from *B. pumilus*  
410 HY1 inhibited *A. flavus* and *A. parasiticus* with an MIC of 50 mg/L (Cho et al., 2009). This  
411 fungitoxicity of iturins has been attributed to membrane permeabilization (Gordillo and  
412 Maldonado, 2012) where osmotic perturbation allows formation of ion-conducting pores as  
413 opposed to the membrane disruption caused by surfactins (Aranda et al., 2005). Based on the  
414 results of the MIC assays of surfactin, iturin A and fengycin against several strains of yeasts and  
415 fungi in this study, iturin A showed the highest antifungal activity against 7 of the 8 indicator  
416 strains with an MIC ranging from 10 to 50 mg/L (Figure 2), which is in agreement to earlier studies  
417 (Carrillo et al., 2003; Cho et al., 2009).

418 The action of fengycin is less known compared with other lipopeptides but it also readily interacts  
419 with lipid layers to alter the permeability of cell membranes (Deleu et al., 2005). Fengycin exhibits  
420 antifungal activity, specifically against filamentous fungi (Vanittanakom et al., 1986). Recently,  
421 fengycin was reported to mediate the cross-kingdom communication between bacteria and fungi

422 (Venkatesh et al., 2022). Fengycin facilitates bacterial invasion into fungal chlamydospores when  
423 comparing the growth of fungal strains and wild type *B. velezensis* or *B. velezensis*  $\Delta fenD$  in a co-  
424 culture system.

425 Different lipopeptides are known to act in an antagonistic or synergistic manner. For example,  
426 surfactins showed antagonistic activity with fengycins (Tao et al., 2011). The MIC of fengycins  
427 against *Rhizopus stolonifer* increased from 0.4 to 2.0 g/L when commercial surfactins were added  
428 (Tao et al., 2011). In contrast, a synergistic effect was found to be in relation to interactions  
429 between iturin A and surfactins. With the addition of iturin A, the haemolytic activity of surfactin  
430 was significantly increased (Maget-Dana et al., 1992).

431 Iturins were more inhibitory than fengycins against *Gibberella zeae*, while the surfactins  
432 demonstrated no activity even at the highest concentration (1  $\mu$ M) tested (Dunlap et al., 2011). In  
433 cocultures of *Trichoderma harzianum* and *B. velezensis*, iturin inhibited *T. harzianum* more  
434 effectively than fengycin and surfactin (Vassilev et al., 2022). Overall, these findings, together  
435 with the MIC test and mass spectrometry analysis of *daqu* samples in this study, indicate that  
436 iturin A produced by *B. velezensis* FUA2155 is likely the main contributor for the higher antifungal  
437 effect of this strain when compared to the two other strains of *Bacillus* (Table 1) (Dunlap et al.,  
438 2011; Vassilev et al., 2022).

439 Bacilli produce fengycins, iturins and surfactins with a variable acyl side chain with a length of  
440 C3 to C13. Analysis of surfactins in food fermentation also indicated the present of different  
441 congeners differing in the length of the acyl side chain (Lee et al., 2012). Ribosomally synthesized  
442 lipopeptides are often specifically acylated with only one fatty acid while nonribosomally  
443 synthesized lipopeptides are usually produced as congener mixtures (Hubrich et al., 2022). Results  
444 of this study suggest that major congeners of surfactin and iturin have an acyl side chain with 10-

445 13 carbon atoms. To date, the formation of different congeners of lipopeptides in food  
446 fermentations has not been described. Moreover, the role of the length of the acyl side chain for  
447 the antifungal activities of different congeners are not completely understood because most  
448 available studies are confounded by the presence of multiple isoforms or multiple lipopeptides in  
449 even purified fractions (Kang et al., 2020; Kourmentza et al., 2021; Wang et al., 2017).

450 Production of antifungal lipopeptides has been described for multiple strains of *Bacillus* isolated  
451 from solid-state fermented products (Lee et al., 2016; Owusu-Kwarteng et al., 2020; Wu et al.,  
452 2021). The substrate for growth of bacilli strongly impacts the overall amount of lipopeptides, and  
453 the relative abundance of different lipopeptides (Hubrich et al., 2022), therefore, studies in  
454 laboratory media do not reliably predict the production of lipopeptides in food fermentations. Only  
455 few investigations, however, detected the presence of these peptides *in situ* during food  
456 fermentation (Chen et al., 2020; Zhang et al., 2014). Surfactin was produced by *Bacillus* spp. in  
457 the Moutai fermentation processes during *daqu* and stacking fermentation stages, but only a minute  
458 fraction carried over with the distillation into the final liquor (Chen et al., 2020).

459 In conclusion, the presence of *Bacillus* spp. in *daqu* fermentation not only affects the production  
460 of amylolytic and proteolytic enzymes in the fermentation process but also impacts the community  
461 composition assembly by production of antimicrobial lipopeptides. Because the bacterial  
462 production of both lipopeptides and of hydrolytic enzymes are dependent on the growth medium  
463 and may be dependent on a social context, studies that use complex re-constituted fermentation  
464 microbiota are necessary to further our understanding of the interaction between strains of *Bacillus*  
465 spp. and fungi and its impact on product quality.

466 **Acknowledgements**

467 We would like to thank Béla Reiz (University of Alberta Mass Spectrometry Facility) for technical  
468 assistance and advice for the analyses of the fermentation samples. In addition, we thank Jing Zhen  
469 and Dr. Randy Whittal (University of Alberta Mass Spectrometry Facility) for their assistance with  
470 the characterization and analyses of peptide fragments. The Natural Sciences and Engineering  
471 Research Council of Canada is acknowledged for financial support through Discovery Grants to  
472 John Vederas and Michael Gänzle. Zhen Li acknowledges scholarship support from the China  
473 Scholarship Council; Michael Gänzle acknowledges support from the Canada Research Chairs  
474 Program.

475 **References**

- 476 Aranda, F.J., Teruel, J.A., Ortiz, A., 2005. Further aspects on the hemolytic activity of the  
477 antibiotic lipopeptide iturin A. *Biochim. Biophys. Acta* 1713, 51–56.  
478 <https://doi.org/10.1016/J.BBAMEM.2005.05.003>
- 479 Black, B.A., Zannini, E., Curtis, J.M., Gänzle, M.G., 2013. Antifungal hydroxy fatty acids  
480 produced during sourdough fermentation: Microbial and enzymatic pathways, and antifungal  
481 activity in bread. *Appl. Environ. Microbiol.* 79, 1866–1873.  
482 <https://doi.org/10.1128/AEM.03784-12>
- 483 Blin, K., Shaw, S., Kloosterman, A.M., Charlop-Powers, Z., Van Wezel, G.P., Medema, M.H.,  
484 Weber, T., 2021. antiSMASH 6.0: improving cluster detection and comparison capabilities.  
485 *Nucleic Acids Res.* 49, W29–W35. <https://doi.org/10.1093/NAR/GKAB335>
- 486 Carrillo, C., Teruel, J.A., Aranda, F.J., Ortiz, A., 2003. Molecular mechanism of membrane  
487 permeabilization by the peptide antibiotic surfactin. *Biochim. Biophys. Acta - Biomembr.*  
488 1611, 91–97. [https://doi.org/10.1016/S0005-2736\(03\)00029-4](https://doi.org/10.1016/S0005-2736(03)00029-4)

489 Chen, Y., Li, K., Liu, T., Li, R., Fu, G., Wan, Y., Zheng, F., 2021. Analysis of difference in  
490 microbial community and physicochemical indices between surface and central parts of  
491 Chinese special-flavor *Baijiu daqu*. *Front. Microbiol.* 11, 3340.  
492 <https://doi.org/10.3389/FMICB.2020.592421/BIBTEX>

493 Chen, Z., Wu, Q., Wang, L., Chen, S., Lin, L., Wang, H., Xu, Y., 2020. Identification and  
494 quantification of surfactin, a nonvolatile lipopeptide in Moutai liquor. *Int. J. Food Prop.* 23,  
495 189–198. <https://doi.org/10.1080/10942912.2020.1716791>

496 Cho, K.M., Math, R.K., Hong, S.Y., Asraful Islam, S.M., Mandanna, D.K., Cho, J.J., Yun, M.G.,  
497 Kim, J.M., Yun, H.D., 2009. Iturin produced by *Bacillus pumilus* HY1 from Korean soybean  
498 sauce (*kanjang*) inhibits growth of aflatoxin producing fungi. *Food Control* 20, 402–406.  
499 <https://doi.org/10.1016/J.FOODCONT.2008.07.010>

500 Cochrane, S.A., Vederas, J.C., 2016. Lipopeptides from *Bacillus* and *Paenibacillus* spp.: a gold  
501 mine of antibiotic candidates. *Med. Res. Rev.* 36, 4–31. <https://doi.org/10.1002/MED.21321>

502 Deleu, M., Paquot, M., Nylander, T., 2005. Fengycin interaction with lipid monolayers at the air–  
503 aqueous interface—implications for the effect of fengycin on biological membranes. *J.*  
504 *Colloid Interface Sci.* 283, 358–365. <https://doi.org/10.1016/J.JCIS.2004.09.036>

505 Deng, Y., Huang, D., Han, B., Ning, X., Yu, D., Guo, H., Zou, Y., Jing, W., Luo, H., 2021.  
506 Correlation: between autochthonous microbial diversity and volatile metabolites during the  
507 fermentation of Nongxiang Daqu. *Front. Microbiol.* 12, 2117.  
508 <https://doi.org/10.3389/FMICB.2021.688981/BIBTEX>

509 Dunlap, C.A., Schisler, D.A., Price, N.P., Vaughn, S.F., 2011. Cyclic lipopeptide profile of three  
510 *Bacillus subtilis* strains; antagonists of *Fusarium* head blight. *J. Microbiol.* 2011 494 49, 603–



511 609. <https://doi.org/10.1007/S12275-011-1044-Y>

512 Fan, B., Chen, X.H., Budiharjo, A., Bleiss, W., Vater, J., Borriss, R., 2011. Efficient colonization  
513 of plant roots by the plant growth promoting bacterium *Bacillus amyloliquefaciens* FZB42,  
514 engineered to express green fluorescent protein. *J. Biotechnol.* 151, 303–311.  
515 <https://doi.org/10.1016/j.jbiotec.2010.12.022>

516 Ferreira, S. da C., Nakasone, A.K., do Nascimento, S.M.C., de Oliveira, D.A., Siqueira, A.S.,  
517 Cunha, E.F.M., de Castro, G.L.S., de Souza, C.R.B., 2021. Isolation and characterization of  
518 cassava root endophytic bacteria with the ability to promote plant growth and control the *in*  
519 *vitro* and *in vivo* growth of *Phytophthium* sp. *Physiol. Mol. Plant Pathol.* 116, 101709.  
520 <https://doi.org/10.1016/J.PMPP.2021.101709>

521 Gänzle, M., 2022. The periodic table of fermented foods: limitations and opportunities. *Appl.*  
522 *Microbiol. Biotechnol.* 106, 2815–2826. <https://doi.org/10.1007/S00253-022-11909-Y>

523 Gänzle, M.G., Ehmann, M., Hammes, W.P., 1998. Modeling of growth of *Lactobacillus*  
524 *sanfranciscensis* and *Candida milleri* in response to process parameters of sourdough  
525 fermentation. *Appl. Environ. Microbiol.* 64, 2616–2623.  
526 <https://doi.org/10.1128/aem.64.7.2616-2623.1998>

527 Gibbons, J.G., Salichos, L., Slot, J.C., Rinker, D.C., McGary, K.L., King, J.G., Klich, M.A., Tabb,  
528 D.L., McDonald, W.H., Rokas, A., 2012. The evolutionary imprint of domestication on  
529 genome variation and function of the filamentous fungus *Aspergillus oryzae*. *Curr. Biol.* 22,  
530 1403–1409. <https://doi.org/10.1016/J.CUB.2012.05.033>

531 Gordillo, A., Maldonado, M.C., 2012. Purification of peptides from *Bacillus* strains with biological  
532 activity, in: *Chromatography and Its Applications*. InTech, pp. 201–225.

533 <https://doi.org/10.5772/36906>

534 He, G., Huang, J., Zhou, R., Wu, C., Jin, Y., 2019. Effect of fortified *daqu* on the microbial  
535 community and flavor in Chinese strong-flavor liquor brewing process. *Front. Microbiol.* 10,  
536 56. <https://doi.org/10.3389/FMICB.2019.00056/BIBTEX>

537 Huang, Y., Yi, Z., Jin, Y., Huang, M., He, K., Liu, D., Luo, H., Zhao, D., He, H., Fang, Y., Zhao,  
538 H., 2017. Metatranscriptomics reveals the functions and enzyme profiles of the microbial  
539 community in Chinese Nong-flavor liquor starter. *Front. Microbiol.* 8, 1747.  
540 <https://doi.org/10.3389/FMICB.2017.01747/BIBTEX>

541 Hubrich, F., Bösch, N.M., Chepkirui, C., Morinaka, B.I., Rust, M., Gugger, M., Robinson, S.L.,  
542 Vagstad, A.L., Piel, J., 2022. Ribosomally derived lipopeptides containing distinct fatty acyl  
543 moieties. *Proc. Natl. Acad. Sci. U. S. A.* 119, e2113120119.  
544 [https://doi.org/10.1073/PNAS.2113120119/SUPPL\\_FILE/PNAS.2113120119.SAPP.PDF](https://doi.org/10.1073/PNAS.2113120119/SUPPL_FILE/PNAS.2113120119.SAPP.PDF)

545 Im, S.M., Yu, N.H., Joen, H.W., Kim, S.O., Park, H.W., Park, A.R., Kim, J.C., 2020. Biological  
546 control of tomato bacterial wilt by oxydifficidin and difficidin-producing *Bacillus*  
547 *methylotrophicus* DR-08. *Pestic. Biochem. Physiol.* 163, 130–137.  
548 <https://doi.org/10.1016/J.PESTBP.2019.11.007>

549 Jin, G., Zhu, Y., Xu, Y., 2017. Mystery behind Chinese liquor fermentation. *Trends Food Sci.*  
550 *Technol.* 63, 18–28. <https://doi.org/10.1016/J.TIFS.2017.02.016>

551 Juck, D., Charles, T., Whyte, L.G., Greer, C.W., 2000. Polyphasic microbial community analysis  
552 of petroleum hydrocarbon-contaminated soils from two northern Canadian communities.  
553 *FEMS Microbiol. Ecol.* 33, 241–249. <https://doi.org/10.1111/J.1574-6941.2000.TB00746.X>

554 Kang, B.R., Park, J.S., Jung, W.J., 2020. Antifungal evaluation of fengycin isoforms isolated from

555 *Bacillus amyloliquefaciens* PPL against *Fusarium oxysporum* f. sp. *lycopersici*. Microb.  
556 Pathog. 149, 104509. <https://doi.org/10.1016/J.MICPATH.2020.104509>

557 Kourmentza, K., Gromada, X., Michael, N., Degraeve, C., Vanier, G., Ravallec, R., Coutte, F.,  
558 Karatzas, K.A., Jauregi, P., 2021. Antimicrobial activity of lipopeptide biosurfactants against  
559 foodborne pathogen and food spoilage microorganisms and their cytotoxicity. Front.  
560 Microbiol. 11, 3398. <https://doi.org/10.3389/FMICB.2020.561060/BIBTEX>

561 Lee, J.H., Nam, S.H., Seo, W.T., Yun, H.D., Hong, S.Y., Kim, M.K., Cho, K.M., 2012. The  
562 production of surfactin during the fermentation of *cheonggukjang* by potential probiotic  
563 *Bacillus subtilis* CSY191 and the resultant growth suppression of MCF-7 human breast  
564 cancer cells. Food Chem. 131, 1347–1354.  
565 <https://doi.org/10.1016/J.FOODCHEM.2011.09.133>

566 Lee, J.Y., Shim, J.M., Yao, Z., Liu, X., Lee, K.W., Kim, H.J., Ham, K.S., Kim, J.H., 2016.  
567 Antimicrobial activity of *Bacillus amyloliquefaciens* EMD17 isolated from *Cheonggukjang*  
568 and potential use as a starter for fermented soy foods. Food Sci. Biotechnol. 2016 252 25,  
569 525–532. <https://doi.org/10.1007/S10068-016-0073-Z>

570 Leite, H.A.C., Silva, A.B., Gomes, F.P., Gramacho, K.P., Faria, J.C., de Souza, J.T., Loguercio,  
571 L.L., 2013. *Bacillus subtilis* and *Enterobacter cloacae* endophytes from healthy *Theobroma*  
572 *cacao* L. trees can systemically colonize seedlings and promote growth. Appl. Microbiol.  
573 Biotechnol. 97, 2639–2651.

574 Li, P., Aflakpui, F.W.K., Yu, H., Luo, L., Lin, W.-T., 2015. Characterization of activity and  
575 microbial diversity of typical types of Daqu for traditional Chinese vinegar. Ann. Microbiol.  
576 65, 2019–2027.

577 Li, T., Li, L., Du, F., Sun, L., Shi, J., Long, M., Chen, Z., 2021. Activity and mechanism of action  
578 of antifungal peptides from microorganisms: a review. *Molecules* 26, 3438.  
579 <https://doi.org/10.3390/MOLECULES26113438>

580 Li, Z., Bai, Z., Wang, D., Zhang, W., Zhang, M., Lin, F., Gao, L., Hui, B., Zhang, H., 2014.  
581 Cultivable bacterial diversity and amylase production in three typical Daqu of Chinese  
582 spirits. *Int. J. Food Sci. Technol.* 49, 776–786. <https://doi.org/10.1111/IJFS.12365>

583 Li, Z., Schottroff, F., Simpson, D.J., Gänzle, M., 2019. The copy number of the *spoVA*<sup>2mob</sup> operon  
584 determines pressure resistance of *Bacillus* endospores. *Appl. Environ. Microbiol.* 85, e01596-  
585 19. <https://doi.org/10.1128/aem.01596-19>

586 Li, Z., Siepmann, F.B., Rojas Tovar, L.E., Chen, X., Gänzle, M., 2020. Effect of copy number of  
587 the *spoVA*<sup>2mob</sup> operon, sourdough and reutericyclin on rony bread spoilage caused by *Bacillus*  
588 spp. *Food Microbiol.* 91, 103507. <https://doi.org/10.1016/j.fm.2020.103507>

589 Liang, N., Dacko, A., Tan, A.K., Xiang, S., Curtis, J.M., Gänzle, M.G., 2020. Structure-function  
590 relationships of antifungal monohydroxy unsaturated fatty acids (HUFA) of plant and  
591 bacterial origin. *Food Res. Int.* 134, 109237. <https://doi.org/10.1016/j.foodres.2020.109237>

592 Liu, J., Chen, J., Fan, Y., Huang, X., Han, B., 2018. Biochemical characterisation and dominance  
593 of different hydrolases in different types of Daqu – a Chinese industrial fermentation starter.  
594 *J. Sci. Food Agric.* 98, 113–121. <https://doi.org/10.1002/JSFA.8445>

595 Maget-Dana, R., Thimon, L., Peypoux, F., Ptak, M., 1992. Surfactin/iturin A interactions may  
596 explain the synergistic effect of surfactin on the biological properties of iturin A. *Biochimie*  
597 74, 1047–1051. [https://doi.org/10.1016/0300-9084\(92\)90002-V](https://doi.org/10.1016/0300-9084(92)90002-V)

598 Marco, M.L., Sanders, M.E., Gänzle, M., Arrieta, M.C., Cotter, P.D., De Vuyst, L., Hill, C.,

599 Holzapfel, W., Lebeer, S., Merenstein, D., Reid, G., Wolfe, B.E., Hutkins, R., 2021. The  
600 International Scientific Association for Probiotics and Prebiotics (ISAPP) consensus  
601 statement on fermented foods. *Nat. Rev. Gastroenterol. Hepatol.* 18, 196–208.  
602 <https://doi.org/10.1038/s41575-020-00390-5>

603 Metzler-Zebeli, B.U., Hooda, S., Pieper, R., Zijlstra, R.T., Van Kessel, A.G., Mosenthin, R.,  
604 Gänzle, M.G., 2010. Nonstarch polysaccharides modulate bacterial microbiota, pathways for  
605 butyrate production, and abundance of pathogenic escherichia coli in the pig gastrointestinal  
606 tract. *Appl. Environ. Microbiol.* 76, 3692–3701. <https://doi.org/10.1128/AEM.00257-10>

607 Nagao, T., Adachi, K., Sakai, M., Nishijima, M., Sano, H., 2001. Novel macrolactins as antibiotic  
608 lactones from a marine bacterium. *J. Antibiot. (Tokyo)*. 54, 333–339.  
609 <https://doi.org/10.7164/ANTIBIOTICS.54.333>

610 Needham, R., Williams, J., Beales, N., Voysey, P., Magan, N., 2005. Early detection and  
611 differentiation of spoilage of bakery products. *Sensors Actuators, B Chem.* 106, 20–23.  
612 <https://doi.org/10.1016/j.snb.2004.05.032>

613 Ongena, M., Jacques, P., 2008. *Bacillus* lipopeptides: versatile weapons for plant disease  
614 biocontrol. *Trends Microbiol.* 16, 115–125. <https://doi.org/10.1016/J.TIM.2007.12.009>

615 Owusu-Kwarteng, J., Parkouda, C., Adewumi, G.A., Ouoba, L.I.I., Jespersen, L., 2020.  
616 Technologically relevant *Bacillus* species and microbial safety of West African traditional  
617 alkaline fermented seed condiments. *Crit. Rev. Food Sci. Nutr.* 62, 871–888.  
618 <https://doi.org/10.1080/10408398.2020.1830026>

619 Robinson, R.J., Fraaije, B.A., Clark, I.M., Jackson, R.W., Hirsch, P.R., Mauchline, T.H., 2016.  
620 Endophytic bacterial community composition in wheat (*Triticum aestivum*) is determined by

621 plant tissue type, developmental stage and soil nutrient availability. *Plant Soil* 405, 381–396.  
622 <https://doi.org/10.1007/s11104-015-2495-4>

623 Röcken, W., Spicher, G., 1993. Fadenziehende Bakterien-Vorkommen, Bedeutung  
624 Gegenmaßnahmen. *Getreide Mehl Brot* 47, 30–35.

625 Rodríguez, A., Rodríguez, M., Luque, M.I., Justesen, A.F., Córdoba, J.J., 2012. A comparative  
626 study of DNA extraction methods to be used in real-time PCR based quantification of  
627 ochratoxin A-producing molds in food products. *Food Control* 25, 666–672.  
628 <https://doi.org/10.1016/J.FOODCONT.2011.12.010>

629 Roongsawang, N., Washio, K., Morikawa, M., 2010. Diversity of nonribosomal peptide  
630 synthetases involved in the biosynthesis of lipopeptide biosurfactants. *Int. J. Mol. Sci.* 2011,  
631 Vol. 12, Pages 141-172 12, 141–172. <https://doi.org/10.3390/IJMS12010141>

632 Sakandar, H.A., Hussain, R., Farid Khan, Q., Zhang, H., 2020. Functional microbiota in Chinese  
633 traditional *Baijiu* and *Mijiu Qu* (starters): a review. *Food Res. Int.* 138, 109830.  
634 <https://doi.org/10.1016/J.FOODRES.2020.109830>

635 Schirawski, J., Perlin, M.H., 2018. Plant–microbe interaction 2017—the good, the bad and the  
636 diverse. *Int. J. Mol. Sci.* 2018, Vol. 19, Page 1374 19, 1374.  
637 <https://doi.org/10.3390/IJMS19051374>

638 Setlow, P., 2006. Spores of *Bacillus subtilis*: their resistance to and killing by radiation, heat and  
639 chemicals. *J. Appl. Microbiol.* 101, 514–525. <https://doi.org/10.1111/j.1365-2672.2005.02736.x>

641 Shahzad, R., Waqas, M., Khan, A.L., Asaf, S., Khan, M.A., Kang, S.-M., Yun, B.-W., Lee, I.-J.,  
642 2016. Seed-borne endophytic *Bacillus amyloliquefaciens* RWL-1 produces gibberellins and

643 regulates endogenous phytohormones of *Oryza sativa*. Plant Physiol. Biochem. 106, 236–  
644 243. <https://doi.org/10.1016/j.plaphy.2016.05.006>

645 Tao, Y., Bie, X. mei, Lv, F. xia, Zhao, H. zhen, Lu, Z. xin, 2011. Antifungal activity and  
646 mechanism of fengycin in the presence and absence of commercial surfactin against *Rhizopus*  
647 *stolonifer*. J. Microbiol. 2011 491 49, 146–150. <https://doi.org/10.1007/S12275-011-0171-9>

648 Vanittanakom, N., Loeffler, W., Koch, U., Jung, G., 1986. Fengycin-a novel antifungal lipopeptide  
649 antibiotic produced by *Bacillus subtilis* F-29-3. J. Antibiot. (Tokyo). 39, 888–901.  
650 <https://doi.org/10.7164/ANTIBIOTICS.39.888>

651 Vassilev, B., Fifani, B., Steels, S., Helmus, C., Delacuvellerie, A., Deracinois, B., Phalip, V.,  
652 Delvigne, F., Jacques, P., 2022. Coculture of *Trichoderma harzianum* and *Bacillus velezensis*  
653 based on metabolic cross-feeding modulates lipopeptide production. Microorg. 2022, Vol.  
654 10, Page 1059 10, 1059. <https://doi.org/10.3390/MICROORGANISMS10051059>

655 Venkatesh, N., Greco, C., Drott, M.T., Koss, M.J., Ludwikoski, I., Keller, N.M., Keller, N.P.,  
656 2022. Bacterial hitchhikers derive benefits from fungal housing. Curr. Biol. 32, 1523-  
657 1533.e6. <https://doi.org/10.1016/J.CUB.2022.02.017>

658 Wang, C.L., Shi, D.J., Gong, G.L., 2008. Microorganisms in Daqu: a starter culture of Chinese  
659 Maotai-flavor liquor. World J. Microbiol. Biotechnol. 24, 2183–2190.  
660 <https://doi.org/10.1007/S11274-008-9728-0/TABLES/5>

661 Wang, Q.Y., Lin, Q.L., Peng, K., Cao, J.Z., Yang, C., Xu, D., 2017. Surfactin variants from  
662 *Bacillus subtilis natto* CSUF5 and their antifungal properties against *Aspergillus niger*. J.  
663 Biobased Mater. Bioenergy 11, 210–215. <https://doi.org/10.1166/JBMB.2017.1665>

664 Wang, Z., Li, P., Luo, L., Simpson, D.J., Gänzle, M., 2018. Daqu fermentation selects for heat-

665 resistant *Enterobacteriaceae* and bacilli. *Appl. Environ. Microbiol.* 84, e01483-18.  
666 <https://doi.org/10.1128/AEM.01483-18>

667 Wu, X., Jiang, Q., Wang, Z., Xu, Y., Chen, W., Sun, J., Liu, Y., 2021. Diversity, enzyme  
668 production and antibacterial activity of *Bacillus* strains isolated from sesame-flavored liquor  
669 Daqu. *Arch. Microbiol.* 203, 5831–5839. [https://doi.org/10.1007/S00203-021-02552-](https://doi.org/10.1007/S00203-021-02552-8/FIGURES/4)  
670 [8/FIGURES/4](https://doi.org/10.1007/S00203-021-02552-8/FIGURES/4)

671 Xiao, C., Lu, Z.M., Zhang, X.J., Wang, S.T., Ao, L., Shen, C.H., Shi, J.S., Xu, Z.H., 2017. Bio-  
672 heat is a key environmental driver shaping the microbial community of medium-temperature  
673 Daqu. *Appl. Environ. Microbiol.* 83, 1550–1567. [https://doi.org/10.1128/AEM.01550-](https://doi.org/10.1128/AEM.01550-17/FORMAT/EPUB)  
674 [17/FORMAT/EPUB](https://doi.org/10.1128/AEM.01550-17/FORMAT/EPUB)

675 Yang, H., Li, Xu, Li, Xue, Yu, H., Shen, Z., 2015. Identification of lipopeptide isoforms by  
676 MALDI-TOF-MS/MS based on the simultaneous purification of iturin, fengycin, and  
677 surfactin by RP-HPLC. *Anal. Bioanal. Chem.* 407, 2529–2542.  
678 <https://doi.org/10.1007/S00216-015-8486-8/TABLES/1>

679 Yuan, J., Zhao, M., Li, R., Huang, Q., Rensing, C., Raza, W., Shen, Q., 2016. Antibacterial  
680 compounds-macrolactin alters the soil bacterial community and abundance of the gene  
681 encoding PKS. *Front. Microbiol.* 7, 01904.  
682 <https://doi.org/10.3389/FMICB.2016.01904/FULL>

683 Zhang, Bo, Xu, L., Ding, J., Wang, M., Ge, R., Zhao, H., Zhang, Bolin, Fan, J., 2022. Natural  
684 antimicrobial lipopeptides secreted by *Bacillus* spp. and their application in food preservation,  
685 a critical review. *Trends Food Sci. Technol.* 127, 26–37.  
686 <https://doi.org/10.1016/J.TIFS.2022.06.009>



687 Zhang, C., Brandt, M.J., Schwab, C., Gänzle, M., 2010. Propionic acid production by  
688 cofermentation of *Lactobacillus buchneri* and *Lactobacillus diolivorans* in sourdough. Food  
689 Microbiol. 27, 390–395. <https://doi.org/10.1016/j.fm.2009.11.019>

690 Zhang, R., Wu, Q., Xu, Y., Qian, M.C., 2014. Isolation, identification, and quantification of  
691 lichenysin, a novel nonvolatile compound in Chinese distilled spirits. J. Food Sci. 79, C1907–  
692 C1915. <https://doi.org/10.1111/1750-3841.12650>

693 Zheng, X.-W., Tabrizi, M.R., Nout, M.J.R., Han, B.-Z., 2011. Daqu- a traditional Chinese liquor  
694 fermentation starter. J. Inst. Brew. 117, 82–90. [https://doi.org/10.1002/j.2050-](https://doi.org/10.1002/j.2050-0416.2011.tb00447.x)  
695 [0416.2011.tb00447.x](https://doi.org/10.1002/j.2050-0416.2011.tb00447.x)

696 Zheng, X.W., Han, B.Z., 2016. *Baijiu* (白酒), Chinese liquor: history, classification and  
697 manufacture. J. Ethn. Foods 3, 19–25. <https://doi.org/10.1016/J.JEF.2016.03.001>

698 Zheng, Y., Zheng, X.W., Han, B.Z., Han, J.S., Nout, M.J.R., Chen, J.Y., 2013. Monitoring the  
699 ecology of *Bacillus* during *Daqu* incubation, a fermentation starter, using culture-dependent  
700 and culture-independent methods. J. Microbiol. Biotechnol. 23, 614–622.

701

702

703 **Figure Legends**

704 **Figure 1.** Heat map of lipopeptide congeners from *B. amyloliquefaciens* Fad We,  
705 *B. amyloliquefaciens* Fad 82, and *B. velezensis* in liquid LB broth samples. Samples were analyzed  
706 via LCMS and the log[signal intensities] are shown in a gradient. The heatmap is representative  
707 of experiments performed in triplicate biological replicates.

708 **Figure 2.** Minimum inhibitory concentration of surfactin (yellow bar), fengycin (green bar) and  
709 iturin A (blue bar) against filamentous fungi and yeasts. Results were presented as means  $\pm$   
710 standard deviation of quadruplicate independent experiments. Significant differences were  
711 determined by t-test and labeled with asterisks: \*,  $P < 0.05$ ; \*\*,  $P < 0.01$ ; \*\*\*,  $P < 0.001$ .

712 **Figure 3.** The pH during the fermentation of the simplified *daqu* model. Different line colors  
713 indicate the different strains inoculated in the *daqu* models: green, *B. amyloliquefaciens* Fad We;  
714 blue, *B. amyloliquefaciens* Fad 82; yellow, *B. velezensis* FUA2155; and gray, control (without  
715 addition of *Bacillus* strain). Different stages of the fermentation are indicated.

716 **Figure 4.** Viable cell counts during incubation of the simplified *daqu* model. Different line colors  
717 indicate different strains inoculated in the *daqu* samples: green, *B. amyloliquefaciens* Fad We;  
718 blue, *B. amyloliquefaciens* Fad 82; yellow *B. velezensis* FUA2155; and gray, no inoculation.  
719 Different stages of the incubation are indicated. Results are presented as means  $\pm$  standard  
720 deviation for five biological replicates.

721 **Figure 5.** Expression of *srfAA*, *fenA* and *ituA* in the samples of the 1<sup>st</sup> (orange bar), 2<sup>nd</sup> (blue bar),  
722 and 3<sup>rd</sup> day (purple bar) of the simplified *daqu* model using *B. amyloliquefaciens* Fad We, *B.*  
723 *amyloliquefaciens* Fad 82 and *B. velezensis* FUA2155. Relative gene expression was quantified by  
724 RT-qPCR with *gyrB* as the housekeeping gene and exponential cultures in LB broth as reference

725 conditions. Significant differences ( $P < 0.05$ ) between the *daqu* model and LB broth conditions  
726 were determined by t-test and labeled with asterisks. Data represent means  $\pm$  standard deviation of  
727 the means from three independent experiment.

728 **Figure 6. (A)** Heat map of lipopeptide congeners produced by *B. amyloliquefaciens* Fad We, Fad  
729 82, and *B. velezensis* FUA2155 in the complex *daqu* model inoculated with 8 bacterial and fungal  
730 strains, and uninoculated control samples. Samples analyzed *via* LCMS and the log[signal  
731 intensities] are shown in a gradient. **(B)** Base structures of antifungal lipopeptide congeners,  
732 denoted by the varying alkyl chain lengths. The heatmap is representative of experiments  
733 performed in triplicate biological replicates.

## Figures and tables

**Table 1.** List of strains used in this study.

Microorganism	Strains and origin	Incubation conditions	Purpose in this study	Reference
<i>Bacillus amyloliquefaciens</i>	Fad We; ropy bread	37 °C, LB	Simplified and complex <i>daqu</i> fermentation	(Röcken and Spicher, 1993)
<i>B. amyloliquefaciens</i>	Fad 82; ropy bread	37 °C, LB	Simplified and complex <i>daqu</i> fermentation	(Röcken and Spicher, 1993)
<i>B. velezensis</i>	<sup>a</sup> FUA2155; <i>daqu</i>	37 °C, LB	Simplified and complex <i>daqu</i> fermentation	(Wang et al., 2018)
<i>Kosakonia cowanii</i>	FUA10121; <i>daqu</i>	37 °C, LB	Complex <i>daqu</i> fermentation	(Wang et al., 2018)
<i>Weissella cibaria</i>	FUA3456; sourdough	30 °C, mMRS	Complex <i>daqu</i> fermentation	
<i>Saccharomyces cerevisiae</i>	FUA4002; sourdough	30 °C, MEA	Complex <i>daqu</i> fermentation and MIC test	
<i>Saccharomycopsis fibuligera</i>	FUA4036; <i>daqu</i> starter	30 °C, MEA	Complex <i>daqu</i> fermentation and MIC test	
<i>Pichia kudriavzevii</i>	FUA4039; <i>daqu</i> starter	30 °C, MEA	Complex <i>daqu</i> fermentation and MIC test	
<i>Aspergillus niger</i>	FUA5001	25 °C, MEA	Complex <i>daqu</i> fermentation and MIC test	(Black et al., 2013; Liang et al., 2020)
<i>Mucor racemosus</i>	FUA5009	25 °C, MEA	Complex <i>daqu</i> fermentation and MIC test	
<i>Penicillium roqueforti</i>	FUA5012	25 °C, MEA	Complex <i>daqu</i> fermentation and MIC test	
<i>A. clavatus</i>	FUA5004	25 °C, MEA	MIC test	
<i>A. clavatus</i>	FUA5005	25 °C, MEA	MIC test	

<sup>a</sup> FUA number, Food microbiology culture collection at the University of Alberta.

**Table 2.** List of primers used in RT-qPCR.

<b>Target</b>	<b>Primer</b>	<b>Sequence (5'-3')</b>
<i>gyrB</i>	<i>gyrB</i> Forward	ATCGTCGACAACAGTATTG
	<i>gyrB</i> Reverse	CTTTATATCCGCTTCCGTC
<i>srfAA</i>	<i>srfAA</i> Forward	GACAAGCGGCGTCATCAATC
	<i>srfAA</i> Reverse	CTGCCACGCATAATTCACCG
<i>fenA</i>	<i>fenA</i> Forward	TGCGGTAAACGGCAAACGG
	<i>fenA</i> Reverse	TCAAGAAGCCATTCAGTTCGCG
<i>ituA</i>	<i>ituA</i> Forward	CCGGCACGATTGATATCGC
	<i>ituA</i> Reverse	CCGGCCTGCTTGATAAAGC

**Table 3.** Degree of the mold growth during the first 4 days of the simplified *daqu* model.

Inoculated strain	Incubation time				
	Day 0	Day 1	Day 2	Day 3	Day 4
Control	-	-	+++	++++	+++++
<i>B. amyloliquefaciens</i> Fad We	-	-	+	+	++
<i>B. amyloliquefaciens</i> Fad 82	-	-	++++	++	+++
<i>B. velezensis</i> FUA2155	-	-	-	-	-

–, no mycelial growth visible; +, small spots of mycelial growth; ++, spots of mycelial growth and conidia; +++, 25-50 % of the surface covered by mycelium; and +++++, more than 50 % of the surface covered by mycelium. The reference pictures for defining the fungal growth are indicated in the Figure S1.

**Table 4.** Antifungal activity of peptides extracted from the complex *daqu* model with different strains of *B. amyloliquefaciens* or *B. velezensis*.

Inoculated strain	Incubation time					
	Day 1	Day 3	Day 6	Day 10	Day 13	Day 16
Control	0	0	0	0	0	0
<i>B. amyloliquefaciens</i> Fad We	3 ± 4	1 ± 1	1 ± 0.5	1 ± 0.5	0 ± 0	0.3 ± 0.5
<i>B. amyloliquefaciens</i> Fad 82	0.3 ± 0.5	2 ± 1.7	1 ± 0.8	1 ± 0	1 ± 0	2 ± 2
<i>B. velezensis</i> FUA2155	3 ± 4	3 ± 1	2 ± 1	1 ± 0	1 ± 0.5	1 ± 2

0: no inhibition; 0-0.9: slight inhibition; 1-1.9: moderate inhibition; 2-2.9: strong inhibition;  $\geq 3$ : significant inhibition. Data represent means  $\pm$  standard deviation of the means from three independent experiment. Experiments were down in triplicate.

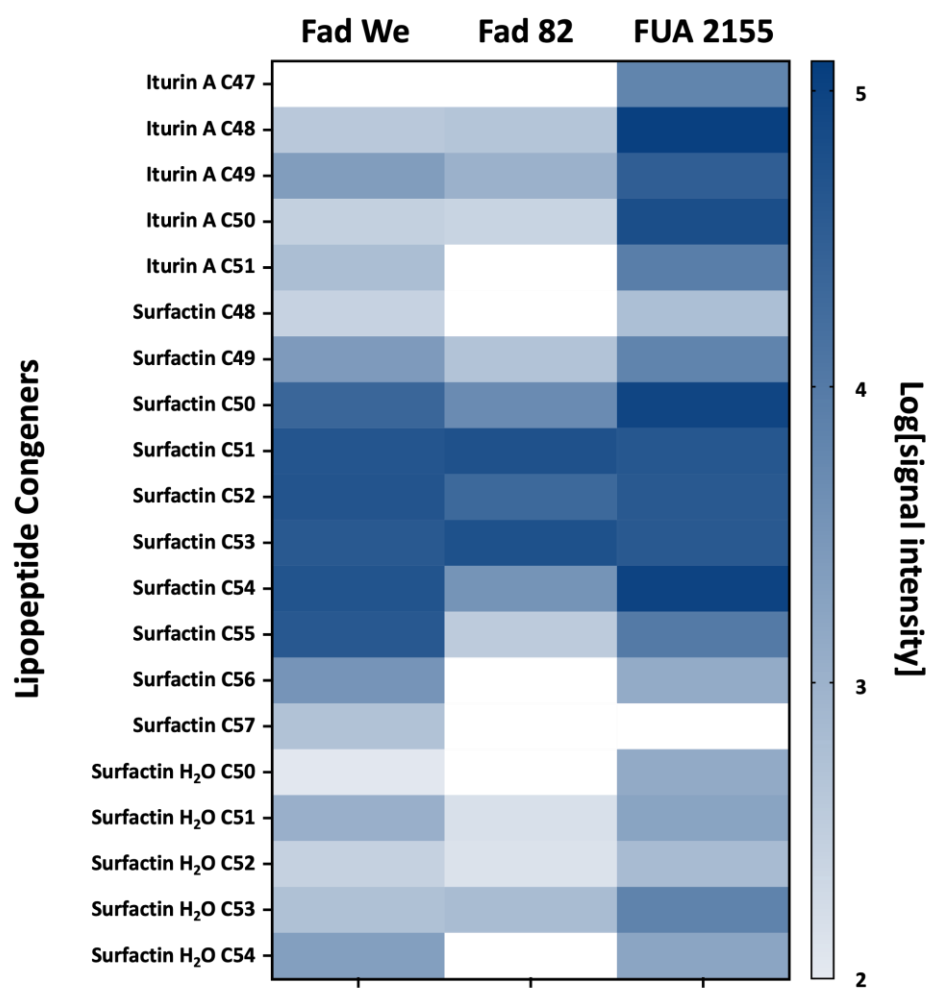
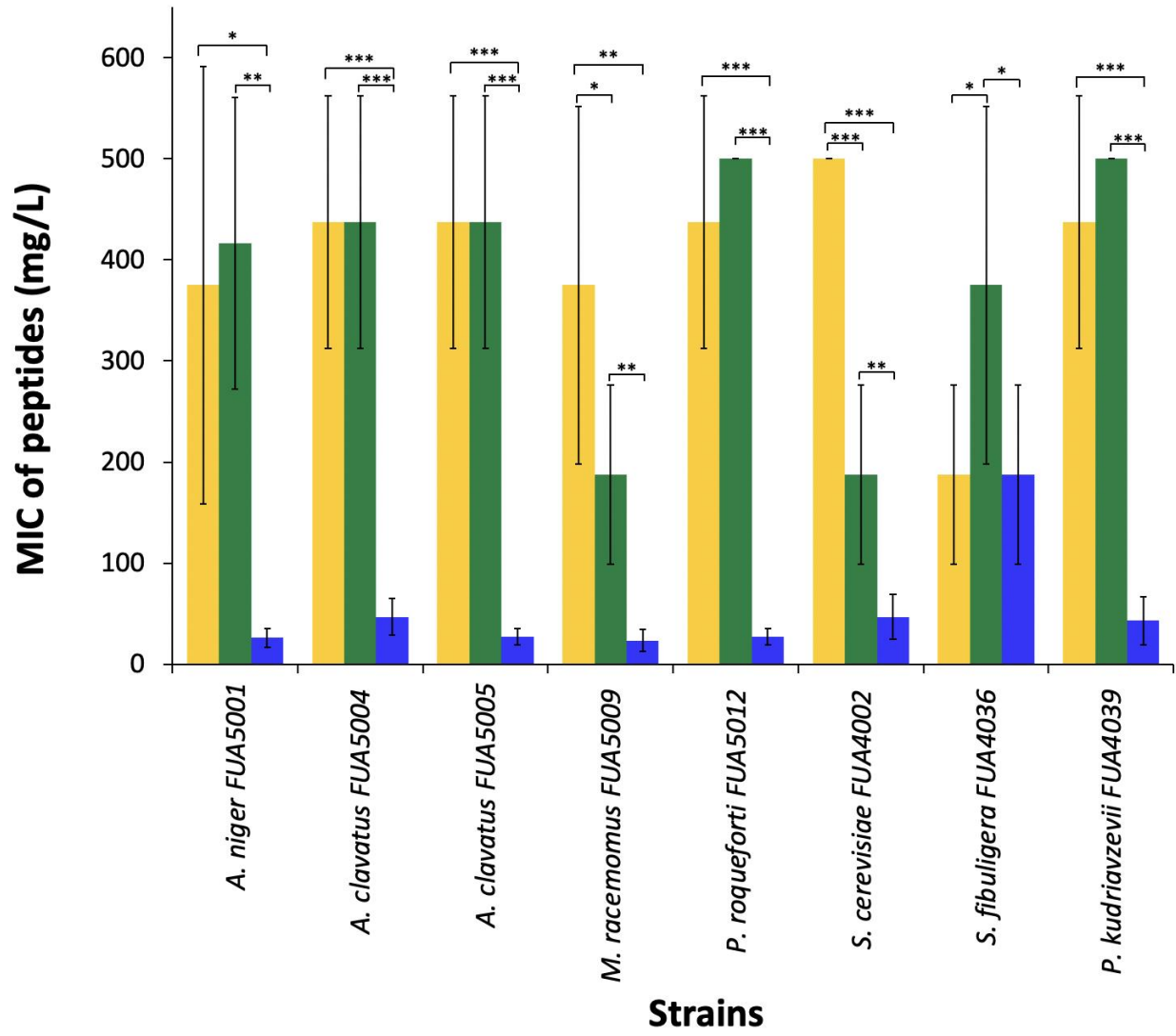


Figure 1.





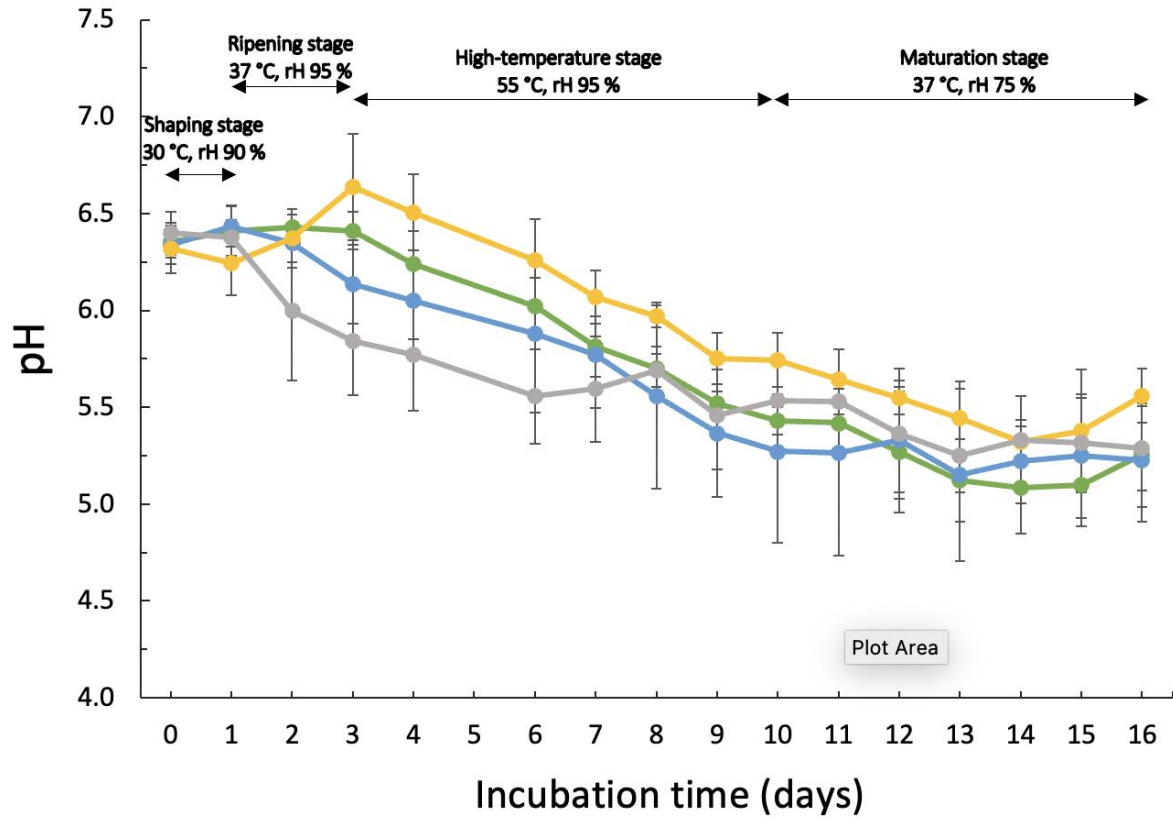
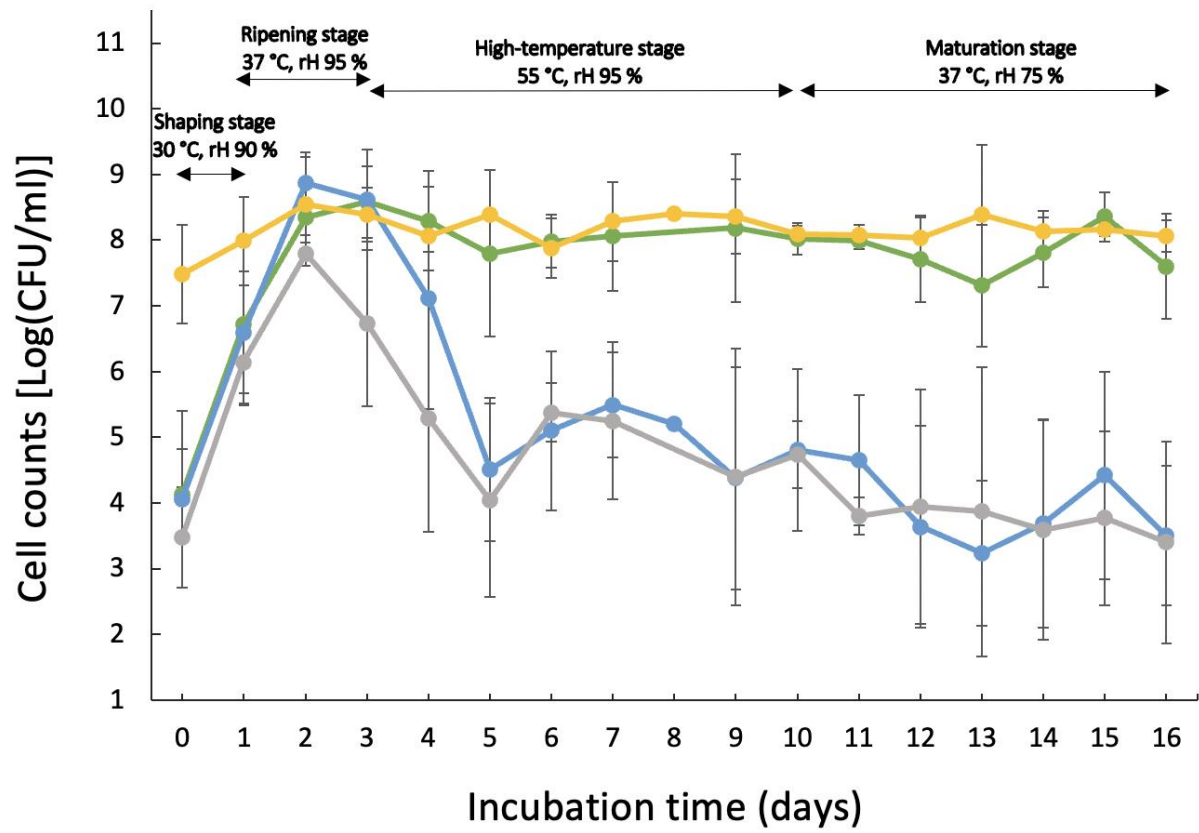
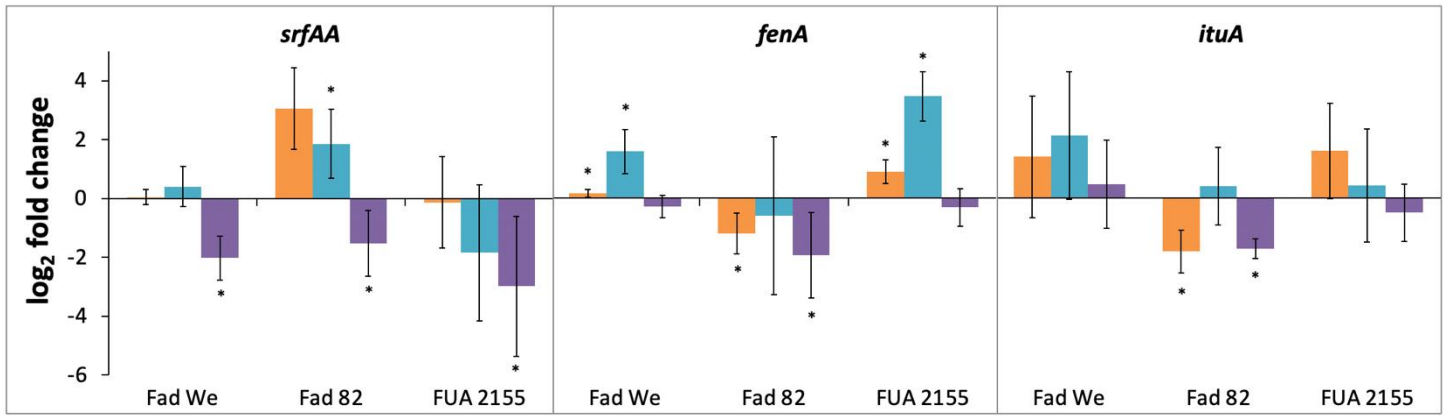
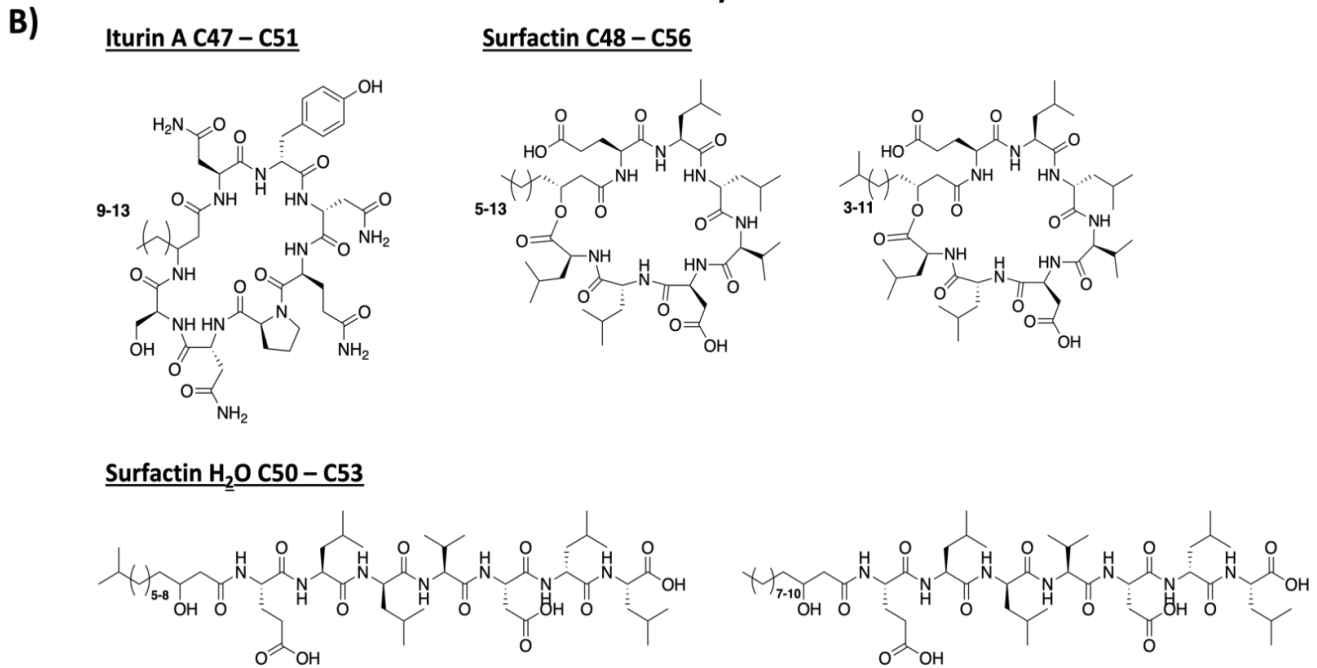
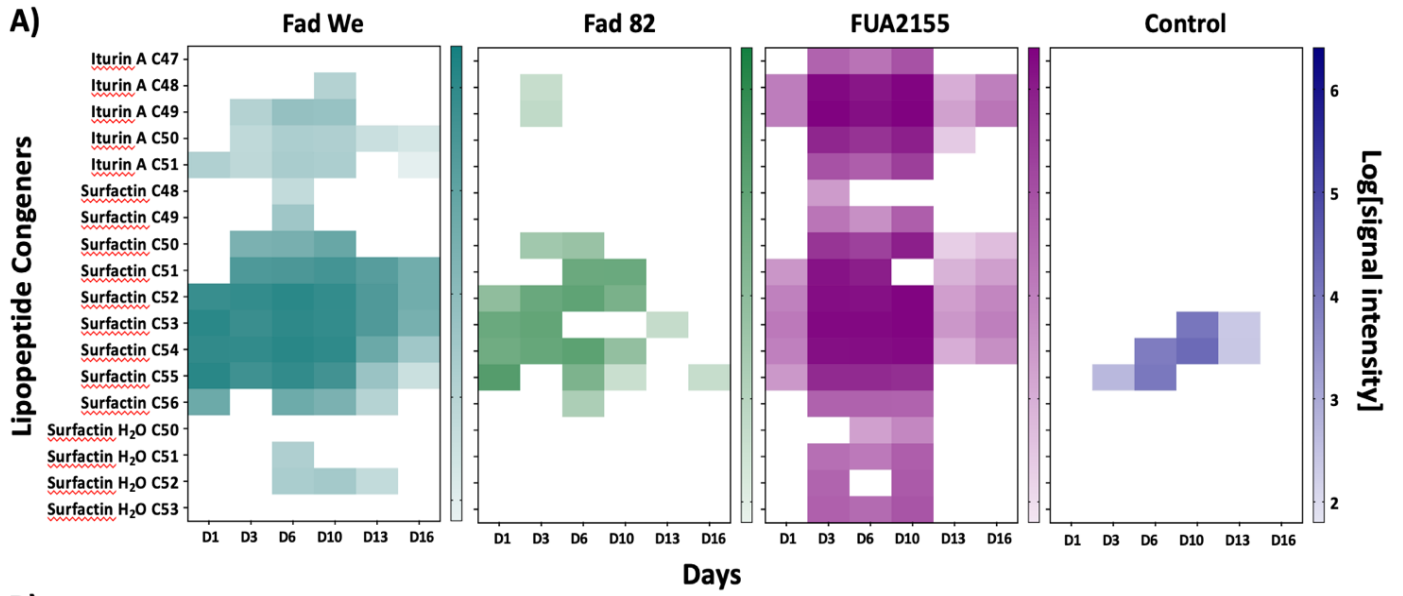


Figure 3.





**Figure 5.**



**Figure 6.**

## Online supplementary material to

### Composition and activity of antifungal lipopeptides produced by *Bacillus* spp. in *daqu* fermentation

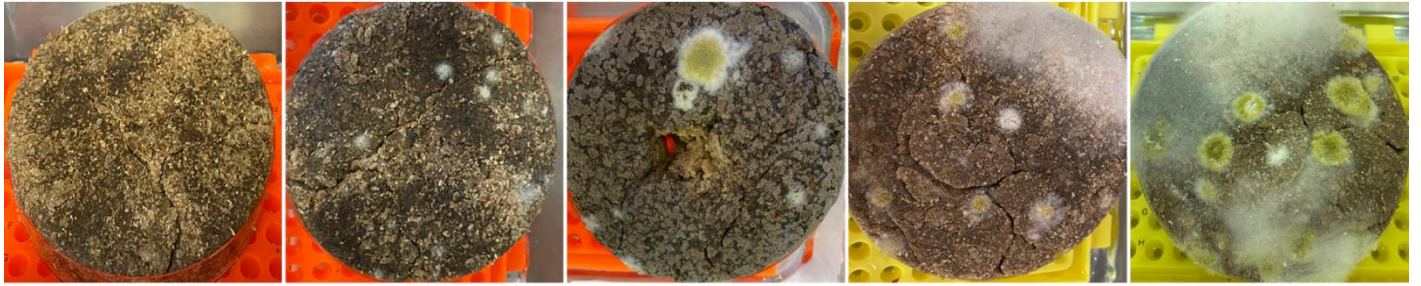
Zhen Li, Kleinberg X. Fernandez, John C. Vederas, Michael G. Gänzle

**Supplementary Figure S1.** Reference pictures for the designation of fungal growth during the simplified *daqu* fermentation model.

**Supplementary Figure S2.** Microbiota analysis by qPCR during the fermentation of the complex *daqu* model samples. **(A)** *Bacillus*. **(B)** Total bacteria. **(C)** Fungi. Different color of the line indicated different strains inoculated in the *daqu* fermentation: green, *B. amyloliquefaciens* Fad We; blue, *B. amyloliquefaciens* Fad 82; yellow *B. velezensis* FUA2155; and gray, no inoculation. The data was based on three replicates of qPCR for one DNA isolation.

**Supplementary Table S1.** Prediction of cluster of different antifungal peptides in the genome of three strains of *Bacillus* predicted by antiSMASH.

**Supplementary Table S2.** Identification of gene clusters encoding different lipopeptides by BLAST.



-

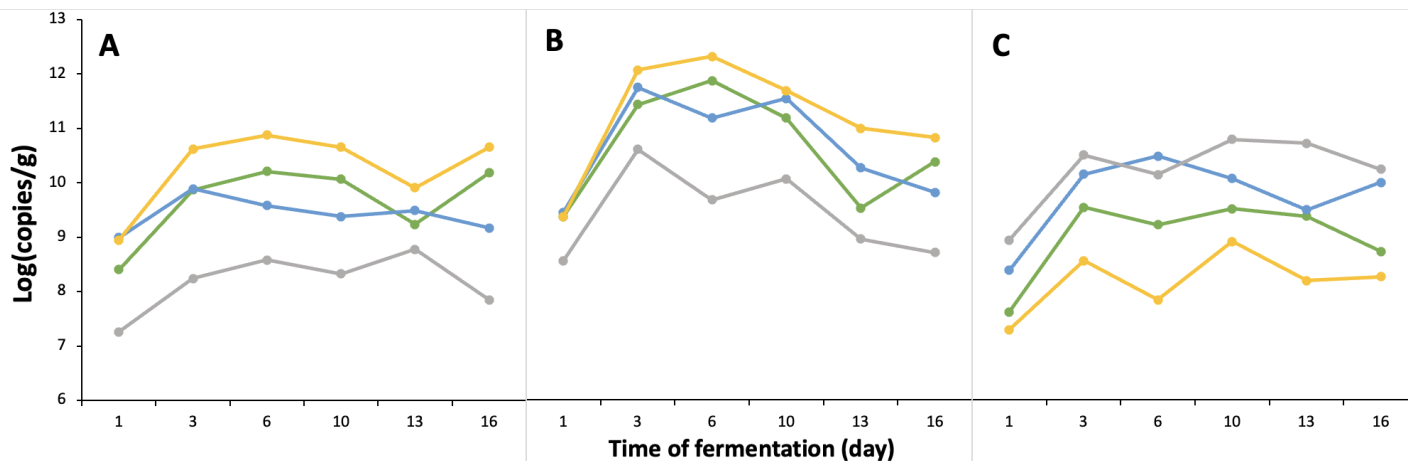
+

++

+++

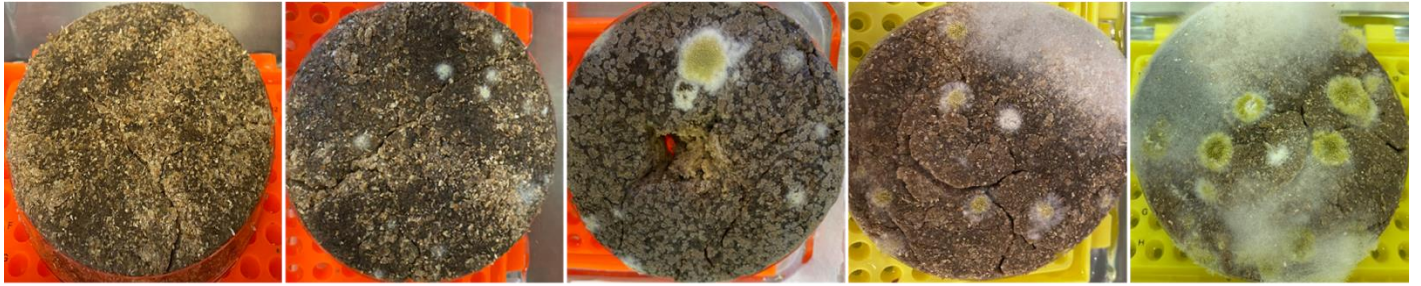
++++

**Supplementary Figure S1** Reference pictures for the designation of fungal growth during the simplified *daqu* fermentation model: -, no mycelial mold growth visible; +, small spots of mycelial growth; ++, spots of mycelial growth and conidia; +++, 25-50 % of the surface covered by mycelium; and +++++, more than 50 % pf the surface covered by mycelium.



**Supplementary Figure S2.** Microbiota analysis by qPCR during the fermentation of the complex *daqu* model samples. **(A)** *Bacillus*. **(B)** Total bacteria. **(C)** Fungi. Different color of the line indicated different strains inoculated in the *daqu* fermentation: green, *B. amyloliquefaciens* Fad We; blue, *B. amyloliquefaciens* Fad 82; yellow *B. velezensis* FUA2155; and gray, no inoculation. The data was based on three replicates of qPCR for one DNA isolation.





-

+

++

+++

++++

**Supplementary Figure S2** Reference pictures for the designation of fungal growth during the simplified *daqu* fermentation model: -, no mycelial mold growth visible; +, small spots of mycelial growth; ++, spots of mycelial growth and conidia; +++, 25-50 % of the surface covered by mycelium; and +++++, more than 50 % pf the surface covered by mycelium.

**Supplementary Table S1.** Prediction of cluster of different antifungal peptides in the genome of three strains of *Bacillus* predicted by antiSMASH.

Secondary Metabolite	Type	Cluster	Similarity		
			Fad We	Fad 82	FUA2155
surfactin	<sup>a</sup> NRP:Lipopeptide	<sup>b</sup> NRPS	82 %	82 %	47 %
surfactin	NRP:Lipopeptide	NRPS	-	-	< 30 %
surfactin	NRP:Lipopeptide	NRPS	-	-	39 %
fengycin	NRP	NRPS, transAT- <sup>c</sup> PKS, betalactone	93 %	93 %	93 %
iturin	NRP, Polyketide	NRPS	77 %	77 %	88 %
bacillaene	transAT-PKS, NRPS, T3PKS	Polyketide + NRP	100 %	100 %	100 %
butirosin A/B	PKS-like	Saccharide	< 30 %	< 30 %	< 30 %
bacilysin	other	Other	100 %	100 %	100 %
bacillibactin	RiPP-like, NRPS	NRP	100 %	100 %	100 %
difficidin	transAT-PKS	Polyketide + NRP	-	-	100 %
Macrolactin H	transAT-PKS	Polyketide	-	-	100 %

<sup>a</sup>NRP: non ribosomal peptides

<sup>b</sup>NRPS: non ribosomal peptide synthetase

<sup>c</sup>PKS: polyketide synthetases

**Supplementary Table S2.** Identification of gene clusters encoding different lipopeptides by BLAST.

Lipopeptides	Accession number	Fad We		Fad 82		FUA2155	
		Query Cover	Per. Ident	Query Cover	Per. Ident	Query Cover	Per. Ident
surfactin	AJ575642.1	91 %	92.89 %	91 %	92.89 %	40 %	98.32 %
fengycin	CP000560.1	56 %	92.83 %	56 %	92.83 %	54 %	97.96 %
iturin	AB050629.1	96 %	90.14 %	96 %	90.14 %	86 %	97.90 %
bacillaene	AJ634060.2	100 %	92.47 %	100 %	92.47 %	100 %	97.98 %
butirosin A/B	AB097196.1	No significant similarity found					
bacilysin	CP000560.1	56 %	92.83 %	56 %	92.83 %	54 %	97.96 %
bacillibactin	AL009126.3	18 %	76.56 %	18 %	76.51 %	29 %	76.36 %
difficidin	AJ634062.2	No significant similarity found		No significant similarity found		100 %	97.88 %
macrolactin H	AJ634061.2	No significant similarity found		No significant similarity found		100 %	98.18 %